THE EFFECT OF DISRUPTED CIRCADIAN RHYTHM AND ASSOCIATED MICRORNA ON BILIARY INJURY AND MALIGNANT TRANSFORMATION

A Dissertation

by

YUYAN HAN

Submitted to the Office of Graduate and Professional Studies of
Texas A&M University
in partial fulfillment of the requirements for the degree of

DOCTOR OF PHILOSOPHY

Chair of Committee,	Gianfranco Alpini
Committee Members,	Cynthia J. Meininger
	Shannon Glaser
	Fanyin Meng
	John Greene
Head of Department,	Van Wilson

December 2014

Major Subject: Medical Sciences

ABSTRACT

Cholangiocarcinoma (CCA) is a devastating tumor characterized by late presentation of symptoms with limited treatment options. Disruption of circadian rhythm is associated with cancer development and progression. MicroRNAs (miRNAs) are a class of small noncoding RNAs that trigger mRNA translation, repression or degradation. The aim of the study was to evaluate the role of deregulated circadian rhythm and related microRNAs in CCA growth. Human intra- and extrahepatic CCA cells and non-malignant (H69) human cholangiocytes were serum starved for 48 hours before stimulation with 50% serum for 2 hours. The 24-hours rhythmic expression of core clock genes, such as Per1/2/3, CLOCK, Bmal1, Cry1/2 and two clock-controlled genes (CCGs) WEE1 and DBP, was evaluated in the selected CCA cells and H69 controls by real-time PCR. To further evaluate the role of Per1, we overexpressed Per1 by transfecting Mz-ChA-1 CCA cells with Per1 or empty vector. In parallel studies, we silenced miR-34a expression with anti-miR-34a inhibitor. Then, we measured: (i) cell proliferation by MTS assays and PCNA immunoblots; (ii) cell cycle; (iii) apoptosis; and (iv) cell migration and. We used luciferase assay to demonstrate whether Per1 acts as a direct target of miR-34a. Finally, we maintained CCA xenograft nude mice in complete dark or light/dark cycle for up to 40 days before evaluating tumor growth. We found the 24-hours rhythmical expression of Per1 was abolished in all CCA cell lines. The rhythmic expression of Bmal1, CLOCK, Per2/3, Cry1/2, WEE1 and DBP was also lost in some of the

CCA cell lines tested. After overexpression of Per1, Mz-ChA-1 showed: (i) reduced cell proliferation; (ii) higher G0/G1 arrest and lower G2/M arrest and (iii) enhanced apoptosis. miR-34a was rhythmically expressed in CCA cell lines and H69. Moreover, the inhibition of miR-34a decreased proliferation, migration and invasion in the selected CCA cell lines. Per1 was verified as a target of miR-34a. However, prolonged darkness therapy did not inhibit the CCA xenograft growth *in vivo*. Summary and conclusions: Disruption of circadian rhythms contributes to the malignant phenotypes of human CCA, and may serve as novel prognostic or therapeutic targets for CCA.

DEDICATION

This dissertation is dedicated to the memory of my beloved father. Though I did not have chance to tell you how much I love you, you are profoundly appreciated for your support to my career pursuit.

This dissertation is also dedicated to my family and many friends. My special gratitude gives to my loving husband, Binbin Zhang for his words of encouragement and support for the whole studies.

ACKNOWLEDGEMENTS

I would like to thank my committee chair, Dr. Gianfranco Alpini, who supported me unconditionally.

I also would like to thank my committee members, Dr. Meininger, Dr. Greene, Dr. Meng, and Dr. Glaser, for their guidance and support throughout the course of this research.

Thanks also go to Dr. Francis and my lab colleagues Julie Venter, Dr. Ray, and Ms. Holly Standeford who helped me on this project.

I also want to extend my gratitude to the Central Texas Veterans Health Care System, Scott & White and the National Institutes of Health for helping fund this project. I also want to express my appreciation to the Central Texas Veterans Health Care System for the lab space and facilities to complete this work.

TABLE OF CONTENTS

Page

LIST OF FIGURES

Page

LIST OF TABLES

CHAPTER I

INTRODUCTION AND LITERATURE REVIEW

Liver and intrahepatic biliary tree

Liver and liver diseases

The liver is the largest solid organ in the human body. The liver secretes bile to help digest fats and stores vitamins (A, D, E and K). The liver is also the processing center and the warehouse for carbohydrates, fats, sugars and vitamins. It helps the body not only to break down hormones, but also detoxify alcohol, drugs and filter waste products from our body. Without the liver, food could not be completely digested, nutrients could not be absorbed and toxic substances could not be removed from our body. The liver is predominantly composed of two kinds of epithelial cells, hepatocytes and cholangiocytes (1). Hepatocytes represent about 70% of the total liver mass, whereas cholangiocytes account for 3% to 5% of the total liver population. Besides these two special epithelia cell types, there is a population called “non-parenchymal cells” in the liver, which also play important roles in liver pathophysiology. These cells include sinusoidal hepatic endothelial cells, Kupffer cells and hepatic stellate cells, etc.

Intrahepatic biliary tree

The intrahepatic biliary epithelium is a three-dimensional (3-D) tubular structure that is lined by biliary epithelia (2). The biliary tree begins with many small branches that end in the common bile duct (also known as the trunk of the biliary tree). The duct, branches of hepatic artery and the portal vein come together to form the central axis of the portal triad (2). The biliary epithelium originates from the biliary pole of hepatocytes that is responsible for the synthesis of canalicular bile. Once produced, the bile is secreted into the lumen of the bile canaliculus, and it moves through the liver lobule in a centrifugal direction. Cholangiocytes modify bile before reaching the duodenum by a series of re-absorptive/secretory events (3), which are modulated by gastrointestinal hormones, neuropeptides and bile acids (4, 5).

Morphological, phenotypic and functional heterogeneity of cholangiocytes

Cholangiocytes are morphologically, phenotypically and functionally heterogeneous (6). In rats, the biliary network is subdivided into two portions according to size differences: the small (≤ 15 μm in diameter) and large (> 15 μm in diameter) bile ducts (7). Large cholangiocytes are more susceptible to damage (8, 9) and respond to secretin via a cAMP-dependent pathway (10), whereas small cholangiocytes are resistant to toxins (8, 9), do not respond to secretin and function by activation of IP_3/Ca^{2+}/PKC-dependent mechanism (11). Secretin, as a gastrointestinal hormone, plays a key role in the event of bile

modification and secretion. It stimulates biliary bicarbonate secretion by interacting with basolateral G protein coupled secretin receptors, which leads to the stimulation of 3'-5'-cyclic adenosine monophosphate (cAMP) and phosphorylation of protein kinase A (PKA), opening of the Cl^- channel, cystic fibrosis transmembrane conductance regulator (CFTR), and subsequent activation of the Cl^-/HCO_3^- anion exchanger 2 (AE2) and bicarbonate secretion into bile (12-15).

Cholangiopathies

Cholangiocytes are the targets of a number of biliary diseases referred as cholangiopathies. Cholangiopathies are characterized by a cholangiocyte-targeted inflammation that leads to bile duct injury/loss coupled with compensatory biliary proliferation in the early stage of liver disease. These biliary diseases include primary biliary cirrhosis (PBC) and primary sclerosing cholangitis (PSC) (1). Chronic biliary injury (due to multiple factors) can induce ductopenia, biliary fibrosis and eventually transform into cholangiocarcinoma.

Cholangiocarcinoma (CCA)

Definition and classification

Cholangiocarcinoma (CCA, also known as bile duct cancer) is a malignant growth composed of mutated epithelial cells that originate from the biliary epithelium. CCA can be divided into two subtypes based on anatomic

location: intrahepatic CCA and extrahepatic CCA. The extrahepatic CCA can be further divided into perihilar CCAs (also known as Klatskin tumors) and distal CCAs, which are divided by the cystic duct. Recently, several studies have shown that CCA may originate from multiple cell types, including hepatocytes, hepatoblasts and hepatic progenitor cells (16, 17).

Cholangiocarcinoma epidemiology

CCA represents the second most common primary liver cancer (18). The overall incidence and mortality rate of intrahepatic CCA appears to have increased worldwide (19). The 5-year survival rate is less than 5%. About 2000 to 3000 people in United States develop CCA each year. Men have a slightly high incidence and mortality of CCA than women. CCA mostly occurs after age 40, except in patients with PSC (20).

Risk factors and diagnosis of CCA

The live flukes *Opisthorchis viverrini* and *Clonorchis sinensis* can cause chronic inflammation in liver and are treated as carcinogens in Southeast Asia. The infection of these liver flukes has been found to be associated with the development of CCA (21, 22). Hepatolithiasis (also known as bile duct stones), which are similar but smaller than gallstones, can also cause inflammation that increases the risk of CCA (21). PSC is the most common pre-existing condition for CCA in western countries. A number of potential risk factors for CCA have

been found in patients with PSC including smoking and alcohol (21). Choledochal cysts are bile-filled sacs that connect with the bile duct. The cells lining the sac are susceptible to carcinogenic changes, which increase the risk of CCA (23). Recently, Hepatitis B and Hepatitis C virus infection and cirrhosis have been found related to CCA (24, 25).

Besides liver and biliary diseases that can increase the risk of CCA, other risk factors have also been found to be correlated with CCA, including inflammatory bowel disease, aging, alcohol, smoking, fatty liver disease (26), and diabetes. In addition, genetic polymorphisms have also been found associated with CCA (26-28).

The symptoms of CCA may be non-specific, making it sometimes difficult for early diagnosis. The symptoms may differ depending on the type of CCA. Extrahepatic CCA symptoms include jaundice, itching, light-colored stools, dark urine, abdominal pain and fever; whereas the intrahepatic CCA is indolent (29). Ultrasound, triple-phase helical computerized tomography are usually used to assess the dilatation of bile duct and possible invasiveness. Magnetic resonance cholangiopancreatography combined with endoscopic retrograde cholangiopancreatography (ERCP) and percutaneous transhepatic cholangiopancreatography (PTC) can provide good sensitivity and specificity in the diagnosis of CCA. Currently, there is no 100% effective biomarker for the early diagnosis of CCA. Carbohydrate antigen 19-9 (CA19-9) only detects 62% of intrahepatic CCA and even less in perihilar CCA (30).

Treatment for CCA and survival rate

As discussed above, due to the difficulty of discovery and diagnosis of CCA, the treatment options for CCA are limited (30). The surgical resection of the tumor is the only effective option for CCA and might increase the long-term survival in some patients (31). However, only the patients who have potentially resectable tumors should undergo surgery. The five-year survival rates vary from 20% to 40% after the surgical resection and poor outcomes are predicted (31, 32). Gemcitabine and cisplatin are standard practice of care for advanced-stage CCA (33). Besides chemotherapy, radiotherapy is also used for patients with non-resectable CCA (34).

Neuroendocrine regulation of CCA growth

Several studies have shown that cholangiocytes synthesize, secrete and respond to neuroendocrine hormones in the course of cholestasis and malignancy transformation (3, 35). For example, serotonin and dopamine secretion is increased in the bile of CCA patients (36). The release of serotonin and dopamine in CCA has been shown to promote the proliferation of CCA, whereas inhibition of serotonin and dopamine inhibits the tumor growth in nude mice (36). Histamine is a biogenic amine that is synthesized by the enzyme, histidine decarboxylase (HDC). Histamine interacts with four G-protein coupled receptors (H1-H4) (37). Previous studies have shown that activation of H3 or H4 receptor inhibits CCA growth by activation of PKCα signaling (37, 38).

Furthermore, silencing of HDC has been shown to inhibit CCA growth both *in vivo* and *in vitro* (39). Histamine release by autocrine or paracrine pathways promotes CCA growth. Melatonin, which is synthesized in pineal gland and peripheral organs, also regulates CCA growth. Melatonin secretion is impaired in CCA patients. Administration of melatonin inhibits CCA growth *in vivo*. In addition, treatment with endothelin (40), caffeic acid phenethyl ester (41), endocannabinoid anandamide (42), gamma-aminobutyric acid (43), and gastrin (44) inhibits CCA growth, whereas leptin (45) and estrogen (46) have been shown to stimulate CCA growth.

Circadian rhythm and cancer development

Circadian rhythms in pathophysiology

Circadian rhythm is a biological process that displays an oscillation of about 24 hours. This circadian clock system is conserved in all organisms and is present not only in the central nervous system but also in peripheral tissues. The circadian clock system signals cells to ensure the optimal timing for physiological activities, which can be synchronized by external signals and persist without these signals. In mammals, the circadian rhythm controls a number of physiologic processes and behavioral patterns, such as the feeding/wake cycle, body temperature rhythms, endocrine rhythms and nutrient update and metabolism (47). The external synchronizing factors include light, hormones, metabolic signals, among which light is the most powerful circadian

signal. Light signals are captured by the retina and transmitted by the retinohypothalamic tract to the suprachiasmatic nucleus (SCN) (48, 49). The SCN, located in the anterior hypothalamus, acts as a master “pacemaker” generating neural and hormonal signals for peripheral clocks through the body (50). Disruption of the circadian rhythm can increase the risk of developing various disorders and diseases including cancer, which is supported by epidemiologic studies on breast, prostate and colorectal cancers (51-53).

Molecular regulation of circadian rhythms

The molecular basis of circadian rhythm is based on a set of clock genes, which include CLOCK (circadian locomotor output cycles kaput), Bmal1 (brain and muscle-Arntlike1), Per1/2/3 (Period 1, 2, and 3), and Cry1/2 (cryptochrome 1-2) (54, 55). Bmal1 and CLOCK, as transcription factors, form a transcription heterodimer complex and bind to the E-box of the promoter region of Period family and Cry family genes, as well as a group of genes called CCGs (clock-controlled genes) (56). The protein products of Per and Cry genes can also negatively regulate the transcription of Bmal1 and CLOCK by forming heterodimers and translocating into the nucleus (54). Other than these core clock genes, there are also other genes and microRNAs involved in the modulation and fine-tuning of the feedback-loop of circadian rhythm to maintain the 24-hours rhythm (57, 58).

Circadian rhythms in the liver

The liver, as the organ responsible for energy homeostasis, has been found directly linked to circadian rhythms via various signaling pathways. Feeding cycles can entrain the liver independently of the SCN and the light cycle, which represents one of the most critical peripheral circadian oscillators. Kornmann *et al* has generated conditional transgenic mice in which Bmal1 transcription is absent only in the liver when the doxycycline-deficient food is supplied. Microarray analysis indicates that about 350 rhythmic genes are abolished in the liver with the absence of doxycycline from the food, suggesting that the liver clock is an important addition to the central clock (59). It is also worthy noting that there are still 31 genes showing a circadian rhythm of expression, indicating the central circadian system could still control part of the liver clock when the local clock is abolished in the liver. Besides this, many hormones related to metabolism, such as glucagon (60), adiponectin (61), insulin (62), leptin (63), corticosterone (64) and ghrelin (65), have been shown to display rhythmical oscillations. In addition, the expression or the activity of metabolic enzymes is also under the control of the circadian clock (66). On the other side, nutrients such as glucose, amino acids, sodium, and ethanol as well as energy levels such as NAD(P)+/NAD(P)H redox can induce or reset the circadian rhythms by modulation of clock gene expression (66).

Loss of circadian rhythmicity of glucose metabolism may lead to metabolic disorders, such as type 2 diabetes. More importantly, by knocking out

core clock genes or inducing point mutation of clock genes, several metabolic disorders were shown in animals (66). For example, *clock*$^{\Delta 19}$ homozygous animals have attenuated diurnal feeding rhythm, obesity, hyperlipidemia, hepatic steatosis and hyperglycemia (67). Similarly, gluconeogenesis is abolished in Bmal1$^{-/-}$ mice. Liver-specific knockout of Bmal1 resulted in loss of rhythmic expression of hepatic glucose regulatory genes (67). Likewise, the glucocorticoid-induced diurnal feeding rhythm is abolished in Per2$^{-/-}$ mice. The Per2$^{-/-}$ mice developed obesity more easily with a high-fat diet as compared with wild type mice (68).

Circadian rhythms and tumorigenesis

As mentioned previously, the circadian clock regulates a group of genes called circadian controlled genes (CCGs). These CCGs are related to different biological functions. Therefore, it is not surprising to find that disrupted circadian rhythms were correlated with cancer development (55). Especially, modern lifestyles result in people being exposed to light longer than before and include more night shifts in their work. Epidemiological studies have indicated the correlation of circadian rhythm with breast cancer incidence (69). There is increasing evidence that the dysregulation of clock genes is related to tumorigenesis. For example, decreased expression of Per1 and Per2 was found in sporadic and familiar breast cancer (70). Methylation of the promoter region of Per1 and Cry1 increased the survival of breast cancer cells (71). Decreased

expression of Per1 was found to be involved in prostate tumorigenesis by inhibiting the transcription activity of the androgen receptor (72). Circadian disruption also facilitates liver carcinogenesis in mice exposed to diethylnitrosamine (DEN) (73).

Epigenetic silencing of Bmal1 in CpG islands causes the loss of circadian rhythmicity and eventually leads to polymphocytic leukemia (74). Suppression of Bmal1 expression increases the metastatic ability of human lung, glioma and prostate cancer. Bmal1regulates the PI3K-MMP2 pathway and cell cycle arrest, which is critical for tumor proliferation and invasion (75). Tissue-specific silencing of Bmal1 could cause insulin resistance (76), reactive oxygen species accumulation, genomic instability, senescence and increased proliferation in epidermal cells (77). Studies have shown that single nuclear polymorphisms in the human *clock* gene are correlated with increased susceptibility to breast, lung, skin, pancreatic, ovarian, colorectal, lymphoma, chronic lymphocyte leukemia and prostate cancers (75).

All tissues and stromal cells have a circadian rhythm-controlled cell cycle, but metastatic cancer cells display arrhythmic or ultradian rhythms of the cell cycle (75). The circadian clock regulates cell proliferation and cancer cell growth by modulating the cell cycle, DNA damage/repair, cellular senescence, metabolic homeostasis and the inflammatory response (75). For example, p53, p21, c-Myc, Mdm2, β-catenin, Cyclin D1, and Wee1 are directly under the control of the circadian clock (78). The activity of β-catenin is regulated directly

by the activation of the Wnt signaling pathway via CKIε. The genes that activate β-catenin include c-Myc, Cyclin D1 and AP1 family members (78). On the other hand, the aberrant expression of β-catenin modulates clock genes by promoting Per2 degradation (79).

Chronotherapy of cancer

Chronotherapy (also known as treatment scheduling) refers to the use of rhythmic cycles in the application of clinic therapy. The idea of chronotherapy, which aims to maximize the efficiency of anticancer treatment by evaluating the biological clocks, was conceived a long time ago. However, it has not been put into reality until recently after more evidence was generated in this area. Recently, the development of programmable time pumps has given hope to the combination chronotherapy protocols that involve multiple anticancer drugs given in a safe and highly effective delivery method. Indeed, a recent meta-analysis has shown that chronotherapy with leucovorin, 5-flurouracil and oxaliplatin has improved the tumor response rate and survival, when compared to conventional chemotherapy delivery in men with colorectal cancer (80). Likewise, chronotherapy protocols with radiation therapy could also improve the therapeutic index. It was found that morning radiation caused more hair loss as compared with evening radiation in mice with a normal dark/light cycle (81). Better anti-tumor efficacy occurred when giving the radiation therapy in the activity phase rather then the rest phase compared with the normal dark/light

cycle (82). Moreover, personalized medication has also shed light on the effects of circadian phase differences in patients (83). The determination of an individual's circadian phase could be achieved by computed acrophase (the time at which the peak of a rhythm occurs) of physical activity, which varies by up to 10 hours among different patients. The monitoring of circadian phase could enable the personalization of chrono-modulated chemotherapy and radiotherapy schedules and optimize the treatment effects (83). However, chronotherapy still has a long way to go before it reaches clinical application. More studies are needed to understand the basic mechanisms underlying the pathophysiology of circadian rhythm and to develop a novel therapy to combine circadian rhythm with different medications to maximize the anti-tumor effect and minimize the toxicity of the medicine.

microRNA and cancer biology

microRNA general background

The microRNAs (miRNAs) are a family of 21-25 nucleotide small non-coding RNAs that can bind to mRNAs to regulate gene expression in a sequence-specific manner. The first miRNA, *lin-4*, was first identified in *C. elegans* in 1993 (84). It did not catch the attention of researchers until the second miRNA, *let-7* (85), was discovered, also in worms, seven years later. The discovery of these two miRNAs provided a completely novel mechanism of gene regulation, also called "post-translational regulation." The latest version of

the miRNA database, June 2014, has 28645 entries of miRNA records. Over 50% of miRNAs are clustered and act redundantly. More than 40% of miRNAs are located in the intronic regions, while ~10% are located in the exonic regions (86). They exert their function by base pairing to partially or completely complementary sites of the target genes and inhibiting their translation. These miRNAs are well conserved between different species. About 55% of C. elegans miRNAs have homologues in humans. The miRNAs in mammals have multiple isoforms (also known as paralogues) (86).

Biogenesis and the target prediction of the miRNAs

The biogenesis of miRNAs initiates from the nucleus and ends in the cytoplasm. They are first transcribed as primary capped and poly-A precursors of miRNA (also known as pre-miRNAs) by RNA polymerase. Then pri-miRNAs form “stem-loop” secondary structures and are cropped by the Drosha/DGCR8 heterodimer enzyme to form the hairpin pre-miRNAs, which are 60-100 nucleotides in length. The pre-miRNAs are then exported into the cytoplasm by Exportin-5 and its partner Ran-GTP. Dicer, an RNase III, then takes the pre-miRNAs and further cleaves them into approximately 22 nucleotide double stranded miRNAs in the nucleus. The miRNA duplex is then recognized by Argonaute (Ago) and forms the RNA-induced silencing complex (RISC), where one strand becomes mature miRNA and the other strand is degraded. The miRNAs then guide Ago to recruit mRNAs by interacting with the target in an

uncomplementary manner. Since miRNAs exert their function through targeting genes, it is important to identify the targets of miRNAs for understanding the specific function of miRNAs. Different computational algorithms have been developed to aid in identifying the potential targets of miRNAs, which are based on conservation criteria (miRanda, PicTar, TargetScan, DIANA-microT) and free energy of binding or secondary structure of 3' UTRs that promote or prevent the RNA bindings (PITA and rna22) (86). However, experimental verification, such as with luciferase reporter assays, is still necessary to confirm the targets of miRNAs.

microRNA in cancer development

While miRNAs play important roles in normal conditions, their dysregulation is found in various diseases, including cancer. A database called miR2Disease summarizes published relationships between miRNA abnormalities and human disease. The research into miRNAs in cancer development started from a finding that miR-15a/16-1 was frequently deleted in chronic lymphocytic leukemia in 2002 (87). From then on, a robust series of studies has been generated aiming to define the roles of miRNAs in tumorigenesis. Several new concepts were raised during the research on roles of miRNAs in oncology.

The first concept involved oncomiRs and tumor-suppressor miRs. These miRNAs are increased or decreased in pathological conditions, allowing them to

act as oncogenes or tumor-suppressors. For example, miR-21 is considered to be an oncogene in HCC, due to its overexpression in HCC (88). On the contrary, *let-7* (89) and miR-26a (90) inhibit tumor progression *in vivo* when systemically administered. Therefore, they are treated as tumor suppressors. Some miRNAs might play a dual role in different cancer types. For example, miR-17-92 cluster acts as an oncomiR in lung, colon, pancreas, and prostate cancers, targeting the 3'UTR of E2F transcription factors to inhibit their translation (91). On the other hand, miR-17-92 cluster also acts as a tumor suppressor in retinoblastoma, breast cancer, HCC and nasopharyngeal carcinoma. Loss of heterozygosity and deletion of the miR-17-92 cluster was observed in these tumors. Finally, miR-17-92 was found to downregulate AIB1 (also known as RAC3, TRAM1 and SRC-3), a proto-oncogenic transcription activator (92).

Another concept is the "miRNome," which is based on the fact that significant changes in miRNA expression in malignant cancer cells compared to their normal controls represents a specific signature in different stages of tumors and different clinical parameters of tumors (93). The miRNA expression profiling in human tumors has defined some signatures that help with diagnosis, staging, progression, prognosis and response to treatment.

Recent findings of microRNAs in cholangiocarcinoma and circadian rhythms

Several studies have proven the direct link between miRNAs and core clock genes. For example, two brain-specific miRNAs, miR-219 and miR-132, are under the control of the CLOCK and Bmal1 heterodimer and show robust circadian rhythm expression (57), whereas silencing miR-219 could regulate the circadian period. Interestingly, miR-132 can be induced by light signals via a MAPK-CREB signaling pathway (57). Specifically in mouse liver, a circadian pattern of miR-122 precursor expression was shown. While transcription of miR-122 was found regulated by REV-ERBα, miR-122 can also target the CCGs, SMARCD1/BAF60a, which specifically regulate hepatic lipid metabolizing genes (94).

A number of miRNAs have been found to be dysregulated in CCA cells, and their targets were related to cell growth and apoptosis. Several studies have shown that miRNAs act as oncomiRs, such as miR-421 (95), miR-21 (88, 96), miR-31 (97) (98), and miR-26 (99), and can regulate cell proliferation via various mechanisms (100). For example, miR-21 was found to target arsenic resistance protein 2 and programmed cell death 4 (PDCD4) and was upregulated in human CCA (101). In contrast, there are a group of miRNAs that act as tumor suppressor miRNAs, such as miR-141 (102-104), miR-138 (105-107), miR-148a (108, 109), miR-152 (110) and miR-370 (100). These miRNAs are downregulated and play an inhibitory role in cell proliferation. Likewise, some

microRNAs contribute to regulation of cell apoptosis and affect drug resistance. For example, miR-320 and miR-204 can regulate Mcl-1 and Bcl-2 expression, respectively, and promote chemotherapeutic-induced apoptosis (111). In addition, because CCAs are frequently developed after a series of pathological alterations from chronic biliary tract inflammation, it is not surprising to see that some miRNAs that are related to inflammation can also play a role during the tumorigenesis of CCA. IL-6 was known to contribute to the uncontrolled proliferation and survival of biliary malignancy through regulating the expression of miR-148a and miR-152 (112). Since a large number of miRNAs, that could target multiple genes and modulate related signal pathways, may be involved in biliary malignancy transformation, it is essential to understand which miRNAs and how these miRNAs contribute to the pathogenesis of CCA for the development of potential prognostic and therapeutic applications.

The Problem

Therefore, evaluating the functional role of miR-34a and its target genes such as Per1 in CCA could provide new insight into interventions for CCA as well as the molecular mechanisms of the disease. The **overall goal** of this dissertation research was to study the role of circadian rhythms, theirrelated miRNAs and the effect of their regulatory pathways on biliary cancer using both *in vivo* animal and *in vitro* cell culture models. These studies provide new evidence of the critical role of core clock genes and their target relationship to

specific miRNA. Modulation of these factors might provide novel prognostic and therapeutic options for clinical application.

CHAPTER II

MATERIALS AND METHODS

Materials

Reagents were purchased from Sigma-Aldrich (St. Louis, MO) unless otherwise indicated. The antibodies were purchased from Santa Cruz Biotechnology (Santa Cruz, CA), unless differently indicated. The miR-34a inhibitors and negative controls were purchased from Ambion Inc. (Austin, Texas). The pCMV6-Per1 and controls were purchased from OriGene (Rockville, MD).

Methods

Cell lines

Six human CCA cell lines (Mz-ChA-1, TFK-1, HuH-28, CCLP, HuCC-T1 and SG-231) of different biliary origin were utilized in our study. Mz-ChA-1 cells (from human gallbladder) were a gift from Dr. G. Fitz (University of Texas Southwestern Medical Center, Dallas, TX) (113); HuH-28 cells (from human intrahepatic bile ducts) (114) and TFK-1 cells (from human extrahepatic bile ducts) (115) were obtained from Cancer Cell Repository, Tohoku University, Japan. These cells were maintained at the conditions previous described (44). CCLP (116), HuCC-T1(117), and SG231(118) (from intrahepatic bile ducts) were a gift from Dr. A.J. Demetris (University of Pittsburgh, PA) and cultured as described (116-118). The human immortalized, nonmalignant cholangiocyte cell

line, H69, (from Dr. G.J. Gores, Mayo Clinic, MN) was cultured as described (119).

Expression of clock genes in nonmalignant and CCA cell lines and human biopsies

The expression and localization of the core clock genes, Bmal1, CLOCK, Per1/2/3 and Cry1/2, was evaluated by immunofluorescence and real-time PCR in the selected CCA lines. For immunofluorescence, cells were seeded onto coverslips and allowed to adhere overnight. Following washing with cold 1x phosphate buffered saline (PBS), the cells on the coverslips were fixed with 4% paraformaldehyde (in 1x PBS) at room temperature for 5 minutes. Cells were permeabilized in PBS containing 0.2% Triton-X100 (PBST), and blocked in 4% goat serum (in PBST) for 1 hour at room temperature. Appropriate dilutions (in 1% goat serum in PBST) of MT1 or MT2 antibodies were added to the coverslips and incubated overnight at 4°C. Cells were washed three times for ten minutes in PBST and a 1:100 dilution (in 1% goat serum in PBST) of a cy3-conjugated secondary antibody (Jackson ImmunoResearch Laboratories, Inc., West Grove, PA) was added for 2 hours at room temperature. Cells were washed three times for ten minutes in PBST and mounted on microscope slides with Prolong® Gold Antifade containing 4,6-diamidino-2-phenylindole (DAPI) as a counterstain (Invitrogen, Carlsbad, CA). Images were taken on an Olympus FluoView 500 laser scan microscope with a DP70 digital camera (Tokyo, Japan).

The expressions of the core clock genes, Bmal1, CLOCK, Per1/2/3, Cry1/2, were evaluated by real-time PCR (120) in H69 and CCA cell lines. RNA was extracted from the selected cell lines using the RNeasy Mini kit (Qiagen, Valencia, CA) and reverse transcribed using the Reaction Ready^{TM} First Strand cDNA Synthesis Kit (SABiosciences, Frederick, MD). These reactions were used as templates for the PCR assays using SYBR Green PCR Master Mix (SABiosciences) in the real-time thermal cycler (ABI Prism 7900HT sequence detection system) using commercially available primers (SABiosciences) designed against human Bmal1 (NM_001178), Per1 (NM_033419), Per2 (NM_022817), Per3 (NM_016831), Cry1 (NM_004075), Cry2 (NM_021117), and CLOCK (NM_004898) and glyceraldeshyde-3- phosphate dehydrogenase (GAPDH, housekeeping gene) (NM_002046) genes. A ΔΔCT (delta delta of the threshold cycle) analysis was performed using H69 as the control sample. Data are expressed as relative mRNA levels ± standard error of the mean (SEM) (n=4). The primer list is provided in Table 1.

We also assessed the expression levels of core clock genes in commercially available Accumax tissue arrays (ISU ABXIS Co., Seoul, Korea) by immunohistochemistry. These tissue arrays contain 48 well-characterized human CCA biopsy samples from different tumor differentiation grades as well as 4 non-malignant liver biopsy samples. Light microscopy and immunohistochemistry observations were taken with a BX-40 light microscope (Olympus, Tokyo, Japan) with a video-cam (Spot Insight, Diagnostic Instrument,

Inc.). Antibodies against Per1 (SC-25362), CLOCK (SC-25361), Bmal1 (SC-48790) and Cry 1 (SC-33177) were utilized for evaluating the expression of these genes in human biopsies. Semi-quantitative analysis was performed. Staining intensity was assessed (in a blinded fashion) using a scale from 1-4 (1 = no staining, 4 = intense staining) and the abundance of positively stained cells was given a score from 1 to 5 (1= no cells stained, 5 = 100% stained). The staining index was given by the staining intensity multiplied by the staining abundance, which gives a range from 1 to 20.

Circadian expression of core clock genes and CCGs in CCA cells and H69

As previously mentioned, even single cells showed circadian expression of clock genes (121). Thus, we demonstrated that nonmalignant and CCA cell lines display different profiles of core clock genes and CCGs rhythmic expression during a 24-hours period. We employed an established *in vitro* synchronization method, as previously described, to detect the 24-hours circadian rhythm in CCA cell lines and cholangiocytes H69 (121). In brief, cells were deprived of serum for 48 hours, and then transferred to a medium containing 50% serum for 2 hours, and then returned to serum-free medium. Cells were harvested every four hours after serum stimulation and evaluated for core clock gene expression (Per1/2/3, Bmal1, Cry1/2), miR-34a and CCG (WEE1, DBP) mRNA expression by real-time PCR as we described previously. The RNA level before serum shock (time 0) of H69 is denoted as 1.

Table 1 List of primers that used in this study

Catalog Number	Gene Symbol	Refseq Accession #	Description
PPH06229F	ARNTL/Bmal1	NM_001178	Aryl hydrocarbon receptor nuclear translocator-like
PPH06231B	CRY1	NM_004075	Cryptochrome 1 (photolyase-like)
PPH06235A	CRY2	NM_021117	Cryptochrome 1 (photolyase-like)
PPH02075A	PER1	NM_002616	Period homolog 1 (Drosophila)
PPH06234E	PER2	NM_022817	Period homolog 2 (Drosophila)
PPH19810B	PER3	NM_016831	Period homolog 3 (Drosophila)
PPH06233A	CLOCK	NM_004898	Circadian Locomotor Output Cycles Kaput
PPH00445A	WEE1	NM_003390	WEE1 homolog (S. pombe)
PPH19697A	DBP	NM_001352	D site of albumin promoter (albumin D-box) binding protein
PPH00216B	PCNA	NM_182649	Proliferating cell nuclear antigen

Restoration of Period 1 expression in Mz-ChA-1 cells

To demonstrate that the restoration of Per1 expression decreases the malignancy of Mz-ChA-1 cells, the 3873-bp of the complete Per1 cDNA-containing C-terminal MYC/DDK tag was cloned into the pCMV-XL expression vector. The predicted expression protein was 136 kDa. The transfection and the selection of clones were performed as previously described (122). The plasmid (1 µg) was transfected by a nucleofector technology (Lonza, Basel, Switzerland) into Mz-ChA-1 cells, according to the manufacturer's instructions. Mz-ChA-1 cells ($1x10^6$ cells per reaction) were resuspended in 100 µl of Nucleofector™ solution (Lonza). Per1 plasmid cDNA (1 µg) was mixed with 100 µl of cell suspension and transferred into a cuvette. The cuvette was inserted into the Nucleofector™ device (Lonza), and the cells were pulsed according to program U-017. After pulsing, the cells were rinsed with pre-warmed complete medium and transferred into a 6-well plate. Culture medium was replaced 24 hours after the transfection. Stable overexpressing Per1 cells were selected based on neomycin resistance. The overexpression of Per1 in Mz-ChA-1 cells was verified by real-time PCR. The cell invasion was evaluated using a cell invasion assay kit (Chemicon international, Temecula, CA).

Evaluation of proliferation, apoptosis, invasion and cell cycle in Mz-ChA-1 cells overexpressing Per1

To evaluate the malignancy features of Mz-ChA-1 cells, we examined the alteration of proliferation, apoptosis and cell cycles in control vector and Per1 cDNA stably transfected cell lines. We detected the proliferation rate by MTS assays, and the expression of PCNA by real-time PCR and western blotting. We evaluated apoptosis and cell cycle using an Annexin V-PE Apoptosis Detection Kit (BD Biosciences, MountainView, CA) (123) and BD Cycletest^{TM} Plus DNA Reagent Kit (BD Bioscience), respectively (124). Briefly, cells used for detecting apoptosis were cultured at 37°C in a CO_2 incubator until cells reached 80% confluence. Then, cells were serum starved for 24 hours. Cells were then harvested and washed with cold 1x PBS twice. Cells were counted and diluted to 1×10^6cells/ml. A cell suspension solution (100 µl) was taken and divided into four polystyrene round-bottom test tubes: (1) unstained control, (2) FITC Annexin V only, (3) PI only and (4) FITC Annexin V + PI. FITC Annexin V and PI (5 µl) were added to the appropriate tubes. The cells were gently vortexed and incubated for 15 minutes at room temperature in the dark. The 1× binding buffer (400 µl) was added to each tube and the tubes were gently vortexed. Cells were analyzed in a BD Accuri ^{TM} C6 flow cytometer with FL1 (FITC) channel and FL 2(PI) channel.

For detecting cell cycle, cells were first serum starved for 48 hours and then changed back to 10% serum for 24 hours. Cells were harvested and

centrifuged (300*g*, 5 min at room temperature). The cell pellet was fixed with cold 70% ethanol. The cells were washed twice with cold PBS and centrifuged (300*g*, 5 min at room temperature). Then, 250 µl Solution A (250 µl) was added, tubes mixed by vortexing and cells incubated for 10 minutes. Then, Solution B (200 µl) was added, tubes mixed by vortexing and cells incubated for another 10 minutes. Finally, 200 µl of cold solution C (PI) was added to each tube, and incubated for 10 minutes in the dark on ice. Samples were then analyzed using a BD Accuri ^{TM} C6 flow cytometer with the FL 2 channel (PI).

To study invasion, we employed the CultureCoat® 96-well BME Cell Invasion Assay Kit (R&D systems, Minneapolis, MN). Briefly, cells were plated and cultured until 80% confluent in a 6-well plate. Then, one day before plating into the 96-well assay kit, cells were put in a serum-free medium. Cells were diluted to 1×10^6 cells/ml in a serum-free medium. Then, 50 µl of diluted cells per well was added to the top chamber and 150 µl of complete medium per well was added to the bottom chamber. After assembling the chamber, the cells were incubated at 37°C in a CO_2 incubator for 48 hours. To evaluate the migration of cells or invasion of cells, 12 µl of Calcein AM was added to 12 ml of cell dissociation solution. The medium was removed from the top chamber and washed with wash buffer and then transferred into a blank black receiver plate. Then, 100 µl of cell dissociation/Calcein AM was added to the bottom chamber and incubated at 37°C in a CO_2 incubator for one hour. The top chamber was

removed before reading the plate at 485 nm excitation and 520 nm emission. Data from control-transfected group was denoted as one.

Aberrantly expressed microRNAs in Mz-ChA-1 cells compared to non-malignant cholangiocytes

To study the miRNAs that were aberrantly expressed in CCA cell lines, we performed a microRNA array using the CCA cell line Mz-ChA-1, and the non-malignant cholangiocyte cell line H69. Total RNA (5µg) was reverse transcribed using a biotin-labeled random octamer oligonucleotide primer. Hybridization of biotin-labeled complementary DNA was done using a custom miRNA microarray chip (ncRNA Program at Center for Targeted Therapy, MD Anderson Cancer Center). The data from these samples, for each cell type, was further analyzed via the BRB-Array Tools software from the National Cancer Institute. A list of aberrantly expressed miRNAs was generated as candidates for further analysis.

Screen candidate microRNAs that target Per1 in CCA

To determine the potential miRNAs that could possibly target Per1, we used three different target prediction programs, DIANA-MicroT v3.0 (http://diana.cslab.ece.ntua.gr/microT/)(125), Miranda (http://www.ebi.ac.uk/enright-srv/microcosm/htdocs/targets/v5/)(126) and RNAhybrid (http://bibiserv.techfak.uni-bielefeld.de/rnahybrid/welcome.html)(127), which use different algorithms. For DIANA-MicroT, we searched for miRNAs that

target Per1 gene (NM_002616) by setting the miTG score at 7. For Miranda, we searched for Per1 as the keyword and picked the *homo sapiens* Per1 (ENST00000354903) for further analysis. With RNAhybrid, we extracted the whole gene from the NCBI nucleotide website (NM_002616.2, 4717 bp) as the mRNA part and the mature miR-34a (UGGCAGUGUCUUAGCUGGUUGU), miR-185 (UGGAGAGAAAGGCAGUUCCUGA) and miR-29b (GCUGGUUUCAUAUGGUGGUUUAGA) as the microRNA part.

The expression of miR-34a was further confirmed by real-time PCR with a Mice MicroRNA Assay Kit (Applied Biosystems, Foster City, CA). The U6 snRNA was used as the endogenous control. A $\Delta\Delta$CT (delta delta of the threshold cycle) analysis was performed using H69 cholangiocytes as controls. Data were expressed as fold-change of relative miRNA levels ± SEM (n=6).

Per1 as a novel target confirmed by luciferase assay in Mz-ChA-1 cells

We performed a luciferase assay to further confirm the suppression of Per1 expression by miR-34a. Mz-ChA-1 cells were plated into 6-well plates and co-transfected with 1 μg of a Renilla luciferase expression construct pRL-TK and 1 μg of the pMIR-PER1-wt-luc or pMIR-PER1-mut-luc firefly luciferase expression construct, along with either miR-34a precursor or control precursor with Lipofectamine® 2000 (Life Technologies, Grand Island, NY). Twenty-four hours later, cells were harvested and plated into 96-well plates at a density of 5000 cells/well. Luciferase assays were performed 24 hours after the cells were

plated into 96-well plates using the dual luciferase reporter assay system (Promega, Madison, WI), as described by the manufacturer. Briefly, 48 hours after transfection, we removed the medium from the cultured cells before washing cells with 1x PBS once. Then, 20 µl of 1× passive lysis buffer was added into the 96-well plate and the 96-well plates were gently shaken for 15 minutes at room temperature. Then, we set up the automated program of the spectrophotometer (Thermo Labsystems , Beverly, MA), and injectors 1 and 2 to dispense 100 µl of LAR II and STOP & GLO® Reagent, respectively. We allowed 2 seconds delay before the measurement and 10 second read time. After dispensing 100 µl of LAR II with injector 1, the firefly luciferase activity was measured to normalize and eliminate background. Then, we dispensed 100 µl of STOP & GLO® Reagent with injector 2 for measuring Renilla luciferase activity. Data were presented as ratio of Renilla/Firefly luciferase activity.

Evaluation of functional role of suppression of miR-34a in cholangiocarcinoma cells

Since miR-34a was found to be increased in CCA cell lines compared to H69 cells and miR-34a can act as both tumor suppressor and oncogene in various tumors (88, 128-131), we wanted to evaluate the functional effect of miR-34a in CCA cells. The miR-34a precursor antisense inhibitor and control (Ambion Inc., Austin, TX) were transfected into Mz-ChA-1 cells and H69 cells with DharmaFECT^{TM} Transfection Reagent (Thermo Scientific, Waltham, MA)

using the standard protocol. Forty-eight hours after transfection, cells were used for evaluation of proliferation, apoptosis and invasion. The silencing of miR-34a was confirmed by miRNA real-time PCR. The cell proliferation was evaluated via MTS assay after silencing of miR-34a in the Mz-ChA-1 cells. The apoptosis was evaluated with the Annexin-V Apoptosis Kit (BD Biosciences Pharmingen, San Diego, CA) and the cell invasion was evaluated using the cell invasion assay kit (Chemicon international), as described above.

Studies in nude mice

Animal procedures were performed under the guidelines of the Baylor Scott and White Institutional Animal Care and Use Committee (IACUC). Male BALB/c nude (nu/nu) mice were kept in a temperature-controlled (20-22°C) environment with 12-hour light-dark cycles and with free access to drinking water and standard mouse chow. Mz-ChA-1 cells (5×10^6) were suspended in 0.25 mL of extracellular matrix gel (Sigma-Aldrich) and injected in the back flank of nude mice. After the tumor was established, mice were randomly divided into two groups: normal 12-hour light-dark cycle group and 24-hours continuous darkness group. Tumor growth was measured three times a week by an electronic caliper, and volume was determined as follows: tumor volume (mm^3) = 0.5 × length (mm) × width (mm) × height (mm). Tumors were allowed to grow until maximum allowable tumor burden was reached, as set forth by the Baylor Scott & White IACUC tumor burden policy. After 42 days, mice were

anaesthetized with sodium pentobarbital (50 mg/kg i.p.) and sacrificed according to institutional guidelines.

Statistical analysis

All data are expressed as mean ± SEM. Differences between groups were analyzed by the Student unpaired t test when two groups were analyzed and by analysis of variance when more than two groups were analyzed, followed by an appropriate *post hoc* test. A p value of <0.05 was considered to indicate statistical significance.

CHAPTER III

RESULTS

Core clock genes were aberrantly expressed in CCA

Expression of core clock genes in CCA cell lines

In order to evaluate whether clock genes were altered in CCA, we first examined the mRNA levels of the core clock genes Bmal1, CLOCK, Per1/2/3, Cry1/2 in intra- and extra-hepatic CCA cell lines as well as the non-malignant control H69 cell line. The mRNA expression of the transcription factor, Bmal1, increased in HuH-28 and CCLP cells compared to H69, but decreased in all of the extra-hepatic cell lines (Mz-ChA-1 and TFK-1 cells) and one intra-hepatic cell line (HuCC-T1) (Figure 1). The expression of CLOCK did not change significantly in Mz-ChA-1 and SG231 cells, but increased about 0.5 fold in HuH-28 and TFK-1 cells. The decreased expression of CLOCK was observed in CCLP and HuCC-T1 cells compared to H69. Then, we examined the negative regulator Period and Cryptochromes family (Figure 2 and Figure 3). The mRNA expression of Per1, significantly decreased in all intra- and extra- hepatic CCA cell lines compared to H69 (Figure 2). Then, we examined other clock genes, including Per2, Per3 and Cry1 and Cry2 in CCA cell lines and H69 cells (Figure 2 and Figure 3). Cry 1 expression increased in all the CCA cell lines except TFK-1 cells (Figure 3), while Cry2 expression decreased in TFK-1 and increased in CCLP compared with H69, but did not show significant changes in the other CCA cells (Figure 1). Per3 expression showed increased expression in HuH-28

and decreased expression in the other CCA cells, except that in CCLP cells, compared with H69 (Figure 2).

In order to analyze the protein coded by core clock genes and the localization of these clock genes, we also measured their expression in CCA cell lines as well as in H69 cells (Figure 4). We showed the expression of Bmal1, CLOCK, Cry1 and Per1 in H69, Mz-ChA-1, TFK-1 and HuCC-T1 cells. Per1 expression slightly decreased in Mz-ChA-1, TFK-1 and HuCCT-1 cells compared with H69, whereas the Cry1 expression was very low in all of the cells examined. CLOCK expression was decreased in TFK-1 and HuCC-T1 compared with H69; there was no significant difference noted in Mz-ChA-1 cells compared with H69. Bmal1 showed increased immunoreactivity in TFK-1, it did not show significant changes in HuCC-T1 and Mz-ChA-1 cells compared to H69.

Expression of core clock genes in human CCA biopsies

Further, we examined by immunohistochemistry the expression of Per1, Bmal1, CLOCK and Cry1 in a human CCA tissue array. There was decreased expression of Per1 in the human CCA biopsies compared to non-malignant controls (Figure 5). The protein level of Bmal1 increased in human CCA biopsies compared to non-malignant control tissues (Figure 5). On the other hand, the expression of CLOCK and Cry1 showed no significant difference compared to non-malignant controls. We also analyzed the core clock gene protein expression in different stages of CCA cells compared with non-malignant

controls. There was no significant stage difference regarding the core clock gene expression compared with non-malignant controls (data not show)

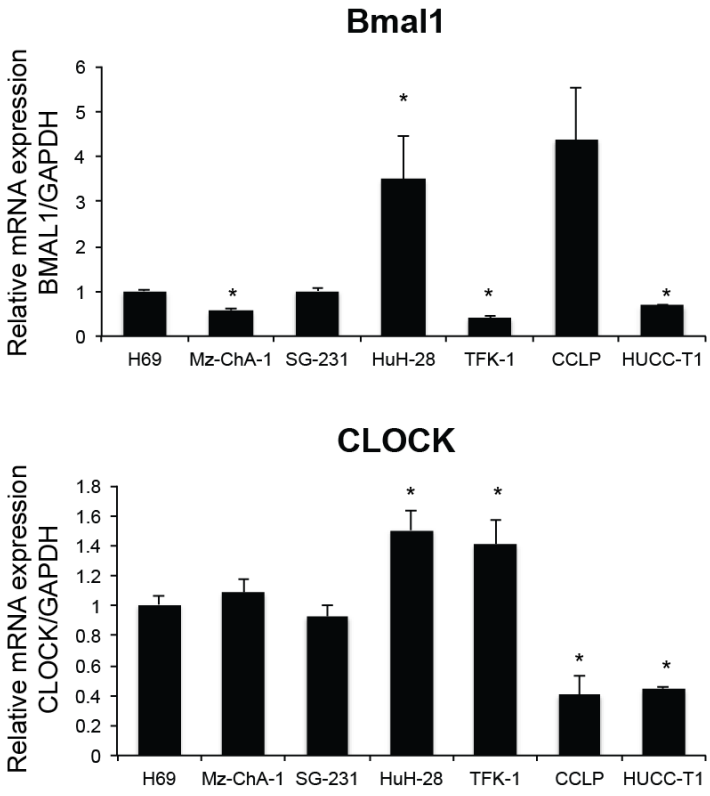

Figure 1 Real-time PCR gene expression of positive feedback loop transcription factors Bmal1 and CLOCK. The gene expression of Bmal1 and CLOCK was measured in six cholangiocarcinoma cell lines and the non-malignant cholangiocyte cell line H69. The gene expression of Bmal1 and CLOCK was upregulated in HuH-28 cells. Bmal1 expression was downregulated in Mz-ChA-1, TFK-1 and HUCC-T1 cells. CLOCK gene expression was downregulated in CCLP and HUCC-T1 cells. Data are mean ± SEM of 3 independent experiments. *p <0.05 vs. Bmal1 and CLOCK mRNA expression of H69 cells.

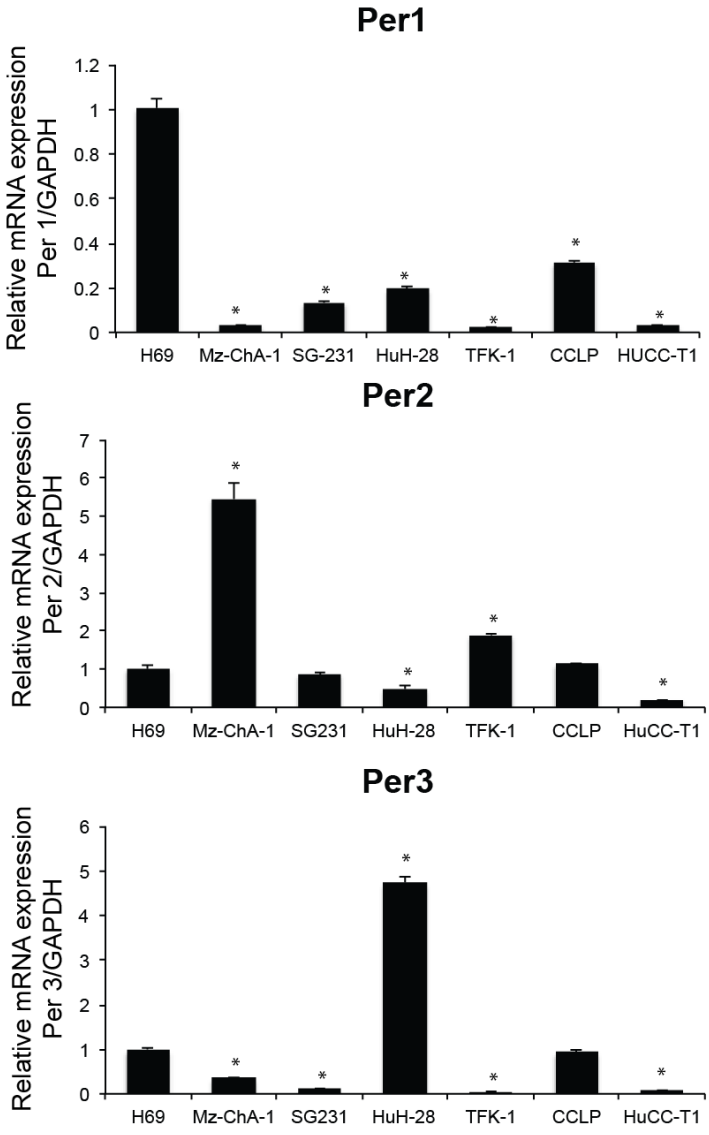

Figure 2 Real-time PCR gene expression of Period family Per1/2/3. The gene expression of Per1, Per2 and Per3 was measured in six cholangiocarcinoma cell lines and the non-malignant cholangiocyte cell line H69. The gene expression of Per1 was downregulated in all CCA cells. Per2 mRNA expression was downregulated in HuH-28 and HUCC-T1 cells, whereas it was upregulated in Mz-ChA-1 and TFK-1 cells. Per3 mRNA expression was upregulated in HuH-28 but decreased in all other CCA cell lines except in CCLP. Data are mean ± SEM of 3 independent experiments. *p <0.05 vs. Bmal1 and CLOCK mRNA expression of H69 cells.

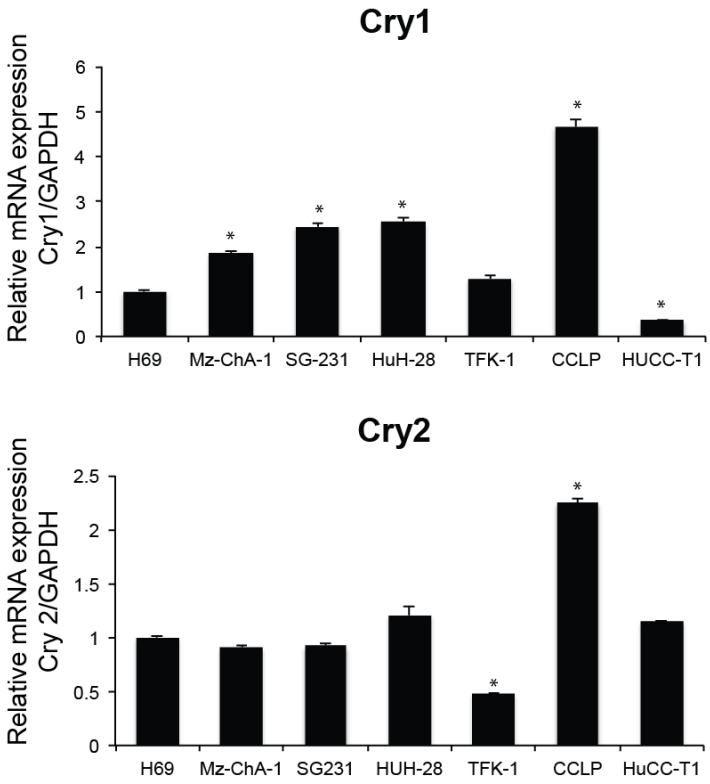

Figure 3 Real-time PCR gene expression of the Cryptochromes family. The gene expression of Cry1 and Cry2 was measured in six CCA cell lines and the non-malignant cholangiocyte cell line. The gene expression of Cry1 was enhanced in all CCA cells except TFK-1 and HUCC-T1. Cry2 mRNA expression did not show significant alteration except an increase in CCLP and a decrease in TFK-1. Data are mean ± SEM of 3 independent experiments. *p <0.05 vs. Bmal1 and CLOCK mRNA expression of H69 cells.

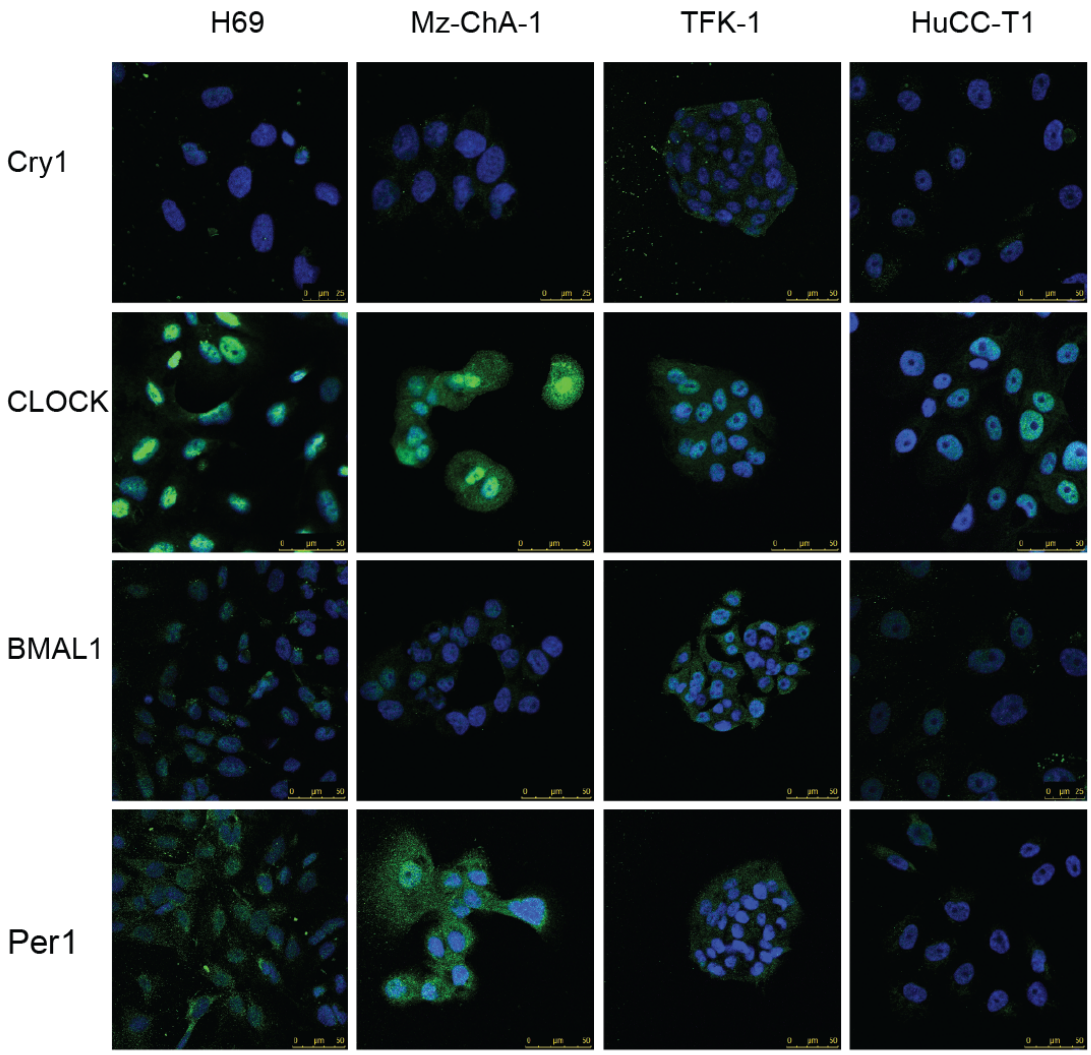

Figure 4 Immunofluorescence images of Cry1, CLOCK, Bmal1, Per1 expression. H69, Mz-ChA-1, TFK-1 and HuCC-T1 cell expression of Cry1, CLOCK, Bmal1 and Per1 was assessed with specific immunoreactivity shown in green and cell nuclei counterstained with DAPI (blue). Negative control consisted of secondary antibody with the absence of primary antibodies (data not shown). All pictures were taken using the same exposure time. As indicated by immunofluorescence, expression of CLOCK did not show significant changes in Mz-ChA-1 and TFK-1, but show decreased reactivity in HuCC-T1 cells. Cry1 staining was very faint in all the cell lines. Whereas Per1 showed a decrease in Mz-ChA-1, TFK-1 and HuCC-T1 cells compared with H69, Bmal1 showed increased immunoreactivity in TFK-1 but didn't show significant changes in HuCC-T1 and Mz-ChA-1 cells compared with H69.

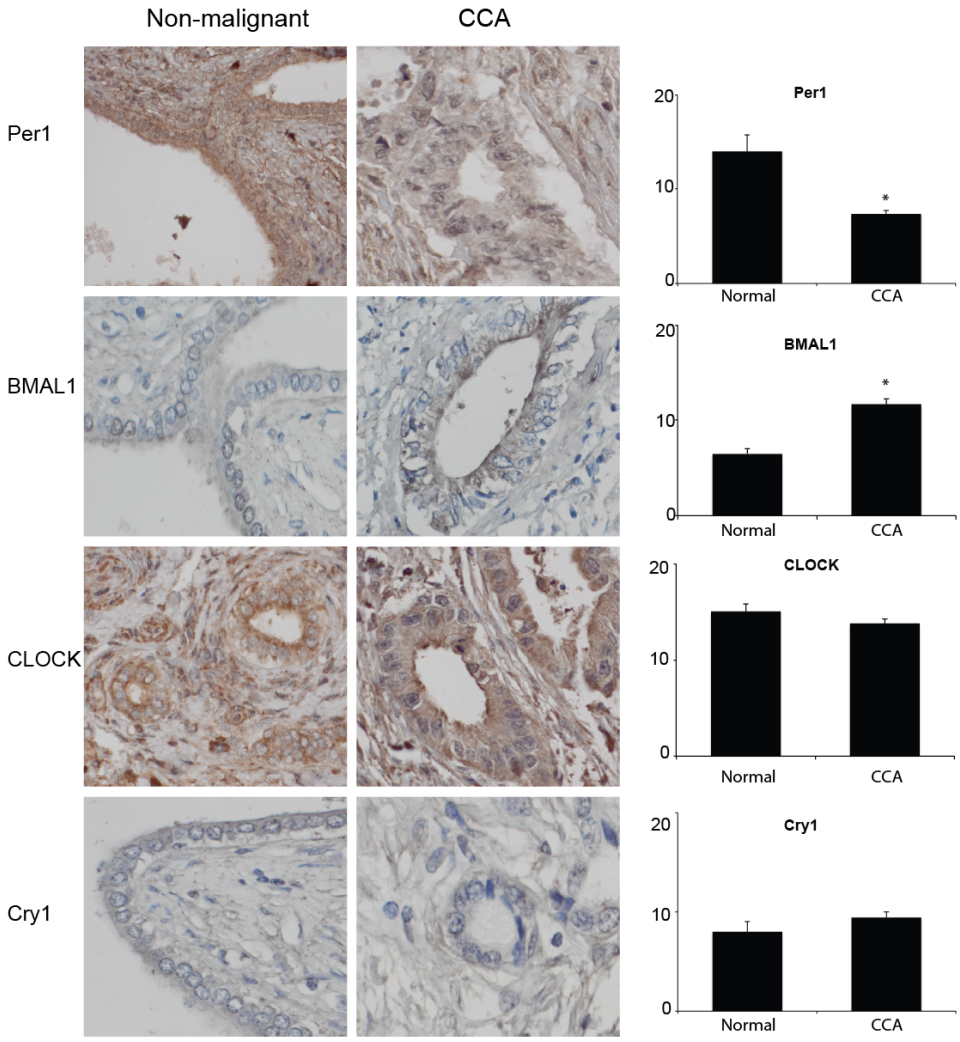

Figure 5 Immunohistochemistry in human biopsies for Per1, Bmal1, CLOCK and Cry1 expression. Per1 immunoreactivity is decreased in CCA samples compared with the non-malignant control, whereas Bmal1 showed enhanced expression in CCA. CLOCK and Cry1 expression was not altered in CCAs. *$p < 0.05$ vs. non-malignant. Data are mean ± SEM of 3 experiments. Original magnification X40.

Disrupted circadian rhythm in CCA cell lines

24-hours circadian expression of Per1 in CCA cell lines and H69

Among the core clock genes we examined for basal level of CCA and non-malignant control expression, Per1 showed the most consistent and significant decreased expression in both human CCA cell lines and biopsies. Previous studies have shown circadian oscillation of clock genes in various cell types *in vitro* via a special synchronization method (121). Therefore, we aimed to evaluate whether the 24-hours rhythmic expression still exists for Per1 expression in CCA lines as compared with H69. As shown in Figure 6, the rhythmic feature of Per1 was present in H69 cell line but was lost in both intra- and extrahepatic CCA cell lines (Figure 6). Specifically, we found the peak expression of H69 at 2 hours and 14 hours after the serum stimulation. Two small peaks can be observed in the TFK-1 cell line at the same time points as in H69.

Rhythmical expression of other clock genes in CCA cell lines and H69

It is worthy to note that all the other core clock genes we examined showed a robust rhythmical expression in H69, whereas circadian rhythms of

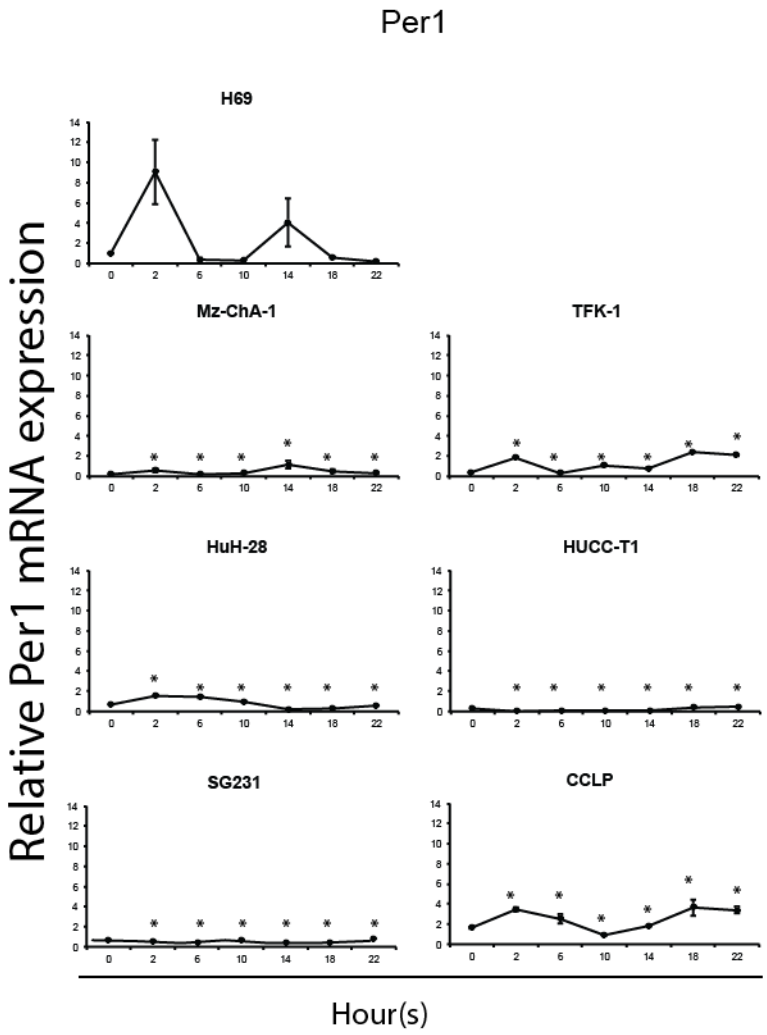

Figure 6 The 24-hours circadian rhythm of Per1 mRNA expression levels in CCA and H69 cell lines. The expression level of Per1 was measured in extra-hepatic CCA cell lines (Mz-ChA-1 and TFK-1), intra-hepatic CCA cell lines (HuH-28, HUCC-T1, SG231 and CCLP) and H69 cells. The cells were stimulated with 50% serum for 2 hours after being serum starved for 48 hours. Samples were taken every four hours until 24 hours. The points represent the mean ± SEM for 3 experiments. *$p < 0.05$ vs. H69 corresponding time points.

these clock genes were lost in some CCA cell lines. Still, they showed phase shift or loss of 24-hours cycle expression in CCA cell lines (Figure 7, Figure 8 and Figure 9). For example, Bmal1 lost circadian rhythm in Mz-ChA-1, TFK-1 and HuCC-T1 cell lines. However, Bmal1 showed rhythmic expression in HuH-28. Furthermore, the phase-shift of Bmal1 was also observed in HuH-28 compared to the H69 cell line. On the other hand, Per2 and Per3 showed rhythmical expression in all extra-hepatic cell lines (Mz-ChA-1 and TFK-1) and the CCLP cell line, which parallels the basal mRNA expression in CCA cell lines, whereas disrupted rhythmical expression of Per2 and Per3 was observed in HUCC-T1, SG231 and HuH-28 (Figure 8). Regarding the Cry1/2 circadian rhythms, Cry1 lost circadian rhythm in HuCC-T1 and SG231 cell lines, but still showed circadian rhythm in Mz-ChA-1 TFK-1 HuH-28 and CCLP cells. While the circadian rhythm still exists for Cry2 expression in TFK-1, HuH-28 and CCLP, it was lost in Mz-ChA1, HuCC-T1 and SG231 cells (Figure 9). From the analysis of these clock genes, we conclude that the CCLP cell line is the one that shows the least disrupted circadian rhythms among the cell lines tested, while HUCC-T1 showed the most disrupted circadian rhythms among these cells (Figure 6, Figure 7, Figure 8 and Figure 9). Among all the core clock genes, Per1, which showed disrupted circadian rhythm, seems more important than other clock genes in the malignant transformation of biliary injury (Figure 6).

Rhythmical expression of clock controlled genes in CCA cell lines and H69

Clock controlled genes (CCGs) are a group of genes that show rhythmical expression under the control of Bmal1/CLOCK heterodimer interaction. Previous studies have found that genes related to metabolism, cell cycle and hormone release are rhythmically expressed in liver (60-62) (64, 65). To assess whether the daily profile of clock-controlled gene expression was affected in CCA cell lines, we also examined the expression of representative CCGs DBP and WEE1 in Mz-ChA-1 and H69 cells. As seen in Figure 10, the 24-hours expression profile of DBP and WEE1 displayed robust rhythmic patterns in H69. But in Mz-ChA-1, the expression of DBP and WEE1 was diminished at all time points. The 24-hours rhythmicity was also lost in this specific CCA cell type.

Restoration of Per1 expression in Mz-ChA-1 cells inhibits the proliferation, apoptosis as well as the invasion features

Inhibition of proliferation in Per1-overexpressing Mz-ChA-1 cells

Since Per1 expression was decreased in all CCA cell lines and lost its rhythmic expression in both intra- and extra CCA cell lines, we next aimed to determine if the restoration of Per1 expression decreases the malignancy of CCA. Expression of Per1 was five fold higher in the selected clone of the stable overexpressing cell line (compared to control), as confirmed by real-time PCR (Figure 11). We found that the proliferation was inhibited at 24 hours, 48 hours and 72 hours as shown in the MTS assay (Figure 12).

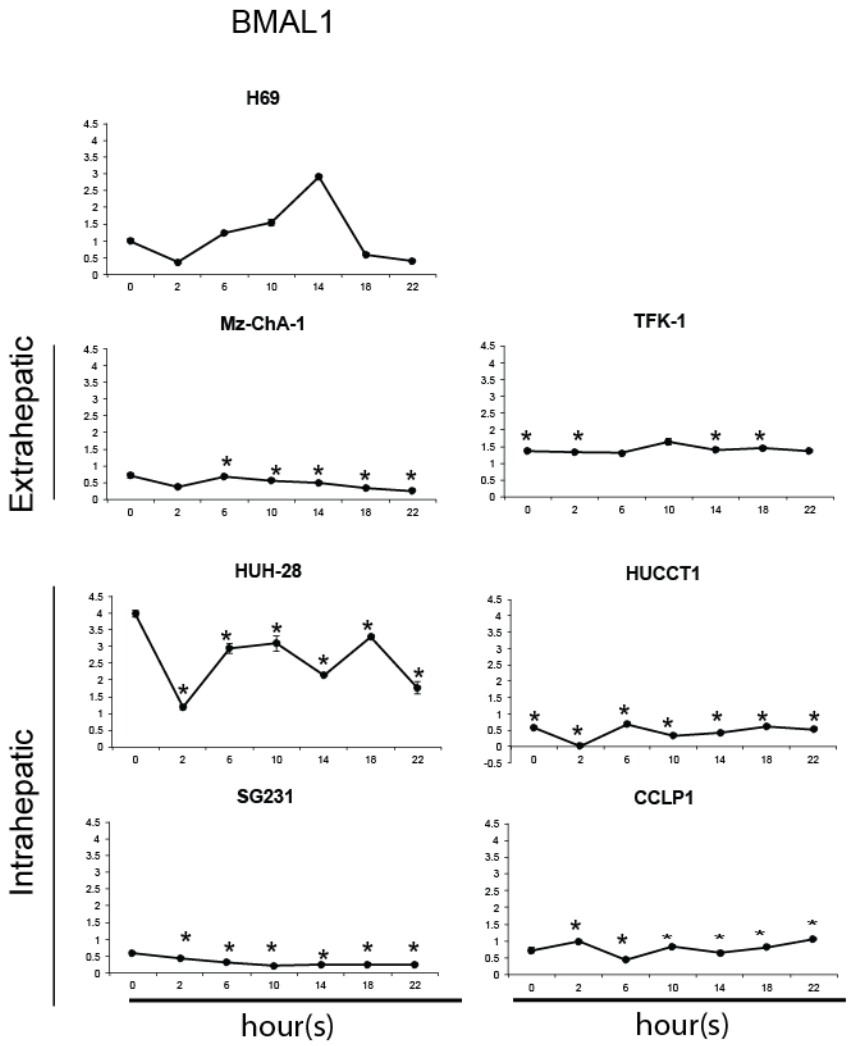

Figure 7 The 24-hours circadian rhythm of Bmal1 mRNA expression levels in CCA and H69 cell lines. The expression levels of Bmal1 were measured in extra-hepatic CCA cell lines (Mz-ChA-1 and TFK-1), intra-hepatic CCA cell lines (HuH-28, HUCC-T1, SG231 and CCLP) and H69 cells. The cells were stimulated with 50% serum for 2 hours after being serum starved for 48 hours. Samples were taken every four hours until 24 hours. The points represent the mean ± SEM for 3 experiments. *$p < 0.05$ vs. H69 corresponding time points.

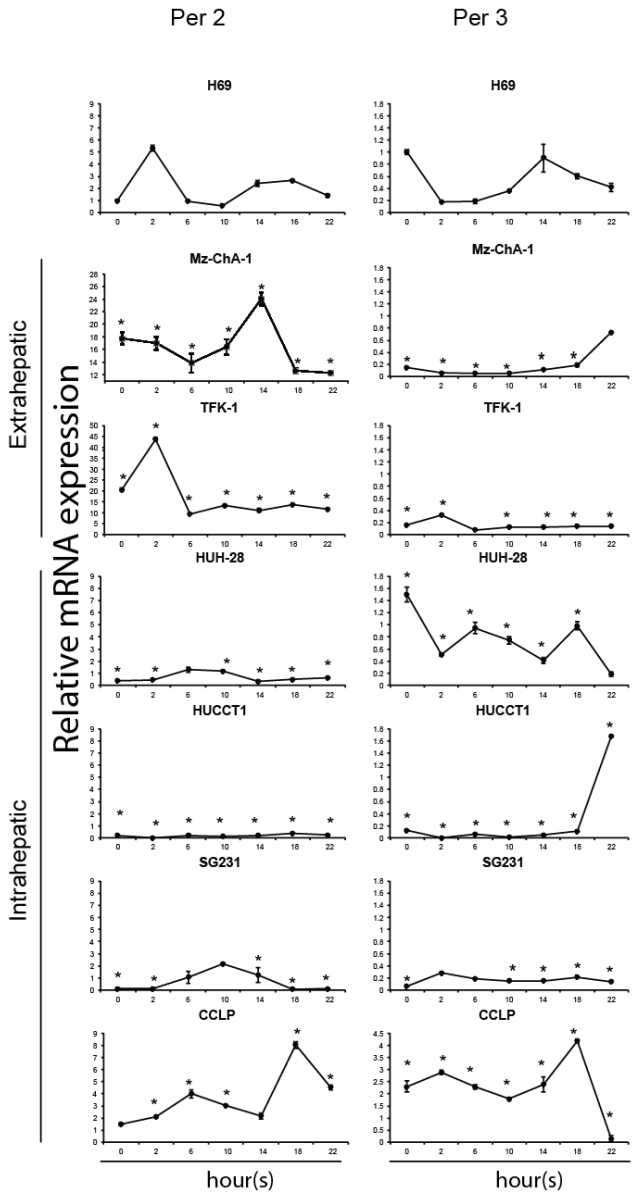

Figure 8 The 24-hours circadian rhythm of Per2 and Per3 mRNA expression levels in CCA and H69 cell lines. The expression levels of Per2 and Per3 were measured in extra-hepatic CCA cell lines (Mz-ChA-1 and TFK-1), intra-hepatic CCA cell lines (HuH-28, HUCC-T1, SG231 and CCLP) and H69 cells. The cells were stimulated with 50% serum for 2 hours after being serum starved for 48 hours. Samples were taken every four hours until 24 hours. The points represent the mean ± SEM for 3 experiments. *$p < 0.05$ vs. H69 corresponding time points.

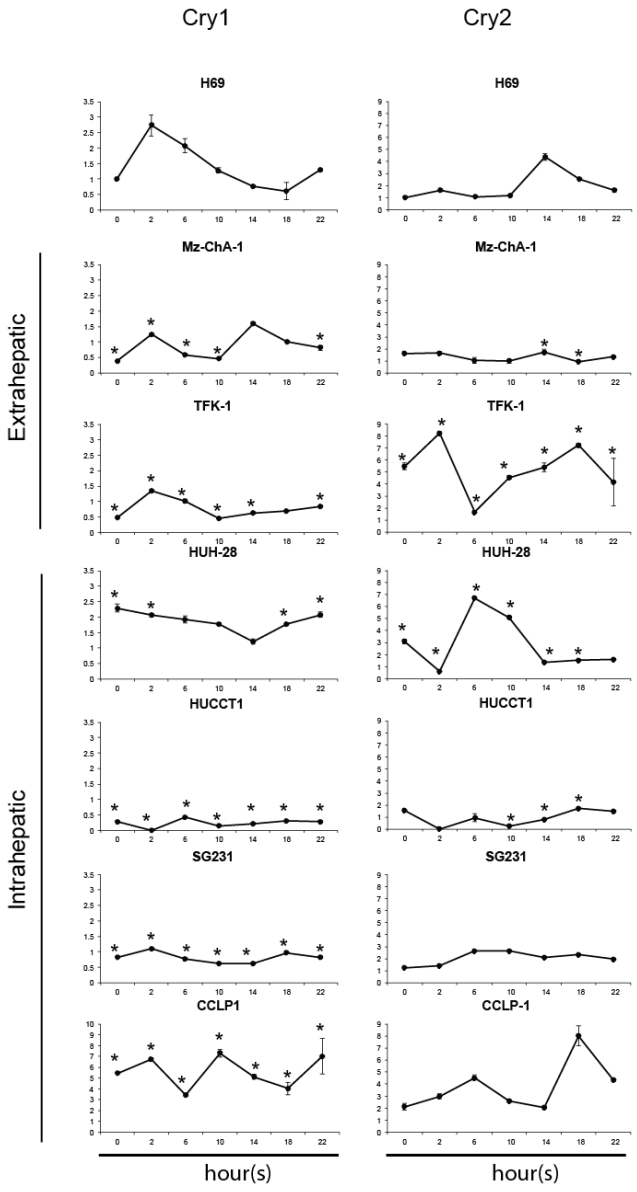

Figure 9 The 24-hours circadian rhythm of Cry1 and Cry2 mRNA expression levels in CCA and H69 cell lines. The expression levels of Cry1 and Cry2 were measured in extra-hepatic CCA cell lines (Mz-ChA-1 and TFK-1), intra-hepatic CCA cell lines (HuH-28, HUCC-T1, SG231 and CCLP) and H69 cells. The cells were stimulated with 50% serum for 2 hours after being serum starved for 48 hours. Samples were taken every four hours until 24 hours. The points represent the mean ± SEM for 3 experiments. *$p < 0.05$ vs. H69 corresponding time points.

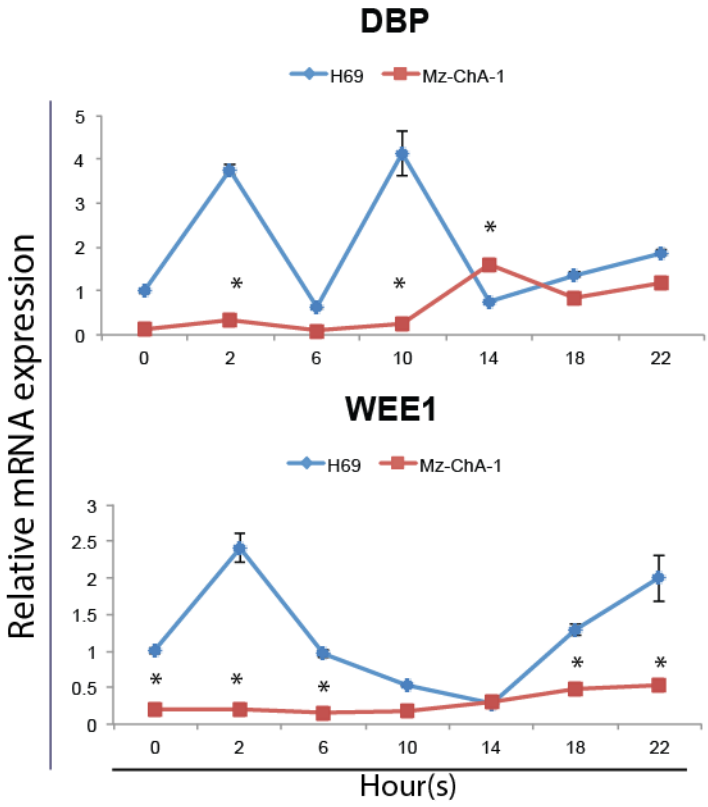

Figure 10 The 24-hours circadian rhythm of known clock-controlled genes CREM, DBP and Wee1 mRNA and their mRNA expression levels in Mz-ChA-1 and H69 cells. The expression levels of CREM, DBP and Wee1 mRNA were measured in Mz-ChA-1 and H69 cells. The cells were stimulated with 50% serum for 2 hours after being serum starved for 48 hours. Samples were taken every four hours until 24 hours. The points represent the mean ± SEM for 3 experiments. *$p < 0.05$ vs. H69 corresponding time points.

We also examined PCNA (proliferation marker) expression by real-time PCR and western blot. Likewise, the expression of PCNA was decreased in two stable Per1-overexpressing (OE) lines (Figure 11 and Figure 12). Per1 can regulate the cell cycle in various tumors (132). Therefore, we examined the cell cycle after overexpressing Per1. As shown in Figure 13, S phase and G2/M phase were inhibited in Per1 OE cells compared with cells transfected with empty vector (EV), whereas the quiescent phase G0/G1 was increased in Per1 overexpressed cells compared with EV. This finding indicates that restoration of Per1 expression inhibits cell proliferation via modulating the cell cycle in Mz-ChA-1 cells.

Enhanced apoptosis in Per1overexpressing cells compared with control in Mz-ChA-1 cells

Furthermore, we found that apoptosis was enhanced, as shown by Annexin V-FITC staining followed by flow cytometry in Mz-ChA-1 cells overexpressing Per1 compared to the control cell line (Figure 14). Briefly, both early apoptosis and late apoptosis were enhanced by restoration of Per1 expression, whereas the percentage of live cells decreased in Per1 OE lines.

Per1 overexpression did not change the invasion or migration of CCA cells

We also studied invasion and migration after overexpression of Per1 in Mz-ChA-1 cells. However, there was no significant difference between Per1 OE and control cell lines regarding the invasion and migration (data not shown).

Aberrant expression of microRNAs (miRNAs) in CCA cells

To study the microRNAs that are dysregulated in CCA, we performed a microRNA array comparing Mz-ChA-1, TFK-1 with H69 cells. A number of miRNAs were found dysregulated in CCA cells (Figure 15). Specifically, a group of miRNAs was upregulated in Mz-ChA-1 cells (cluster 1 in Figure 15), including miR-200b, miR-141, miR-34a, miR-23a, miR-21, miR-27a, miR-222, miR-205 and miR-24-1 (Figure 16). In addition, a group of miRNAs was found to be upregulated in TFK-1 cells as compared to H69 cells, including miR-141, miR-181 family, miR21, let-7, miR-292, miR-200b, miR23a, miR-34 family, miR-215, miR-27 and miR-144 (Lower panel, Figure 16). miR-141, miR-34 family, miR-21, miR-27a and miR-200b were found to be upregulated in both Mz-ChA-1 and TFK-1 cells, indicating that these miRNAs might be important in mediating the malignant transformation of CCA cells.

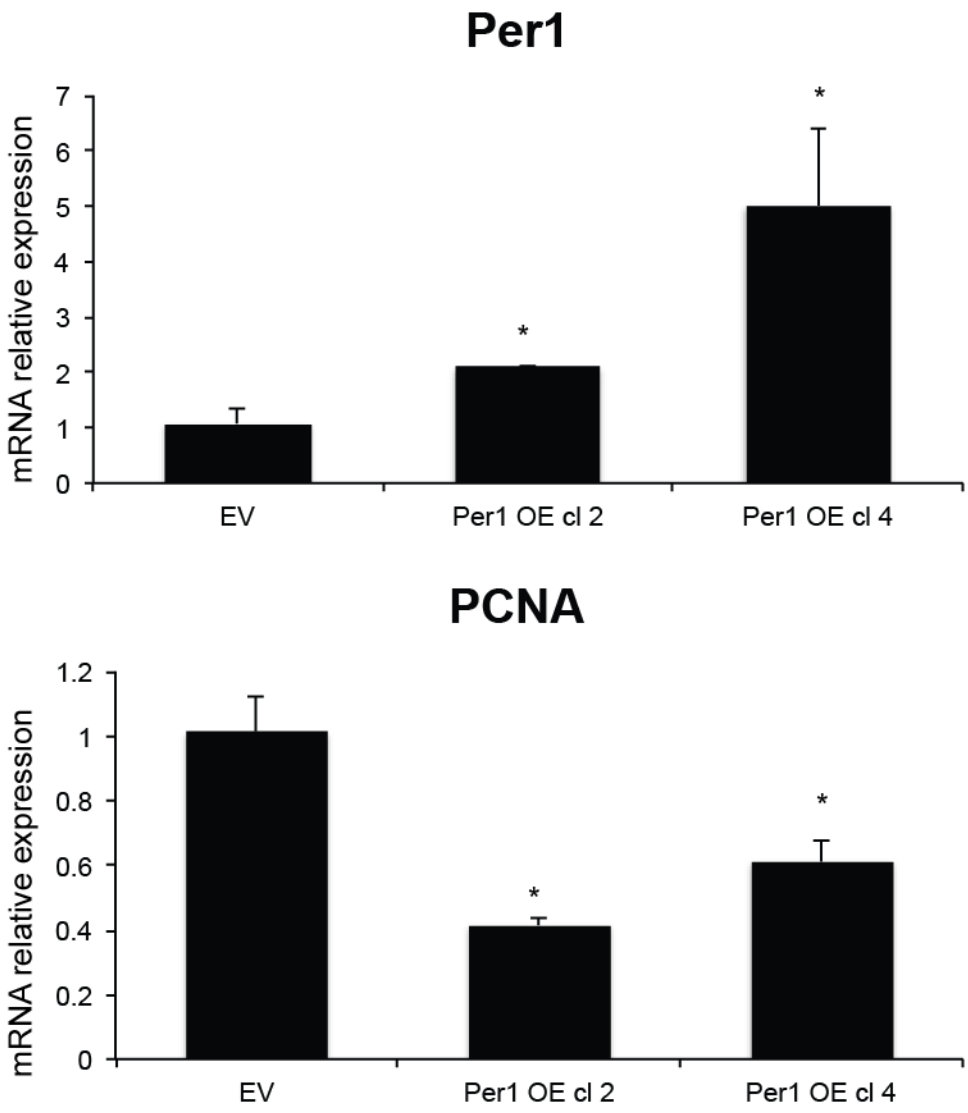

Figure 11 Confirmation of Per1 overexpression and mRNA exprssion of PCNA in Mz-ChA-1 cells. Mz-ChA-1 cells were transfected with empty vector (EV) and Per1 cDNA plasmid and stable transfected clones selected using geneticine. We successfully got two clones overexpressing (OE) Per1: Per1 OE cl 2 and Per1 OE cl 4. The mRNA expression of Per1 was confirmed by real-time PCR. Expression of the proliferation marker PCNA was examined by real-time PCR, which showed reduced expression in both clones. The points represent the mean ± SEM for 4 experiments. *$p < 0.05$ vs. EV. EV=empty vector Per1 OE cl = Per1 overexpressing clones.

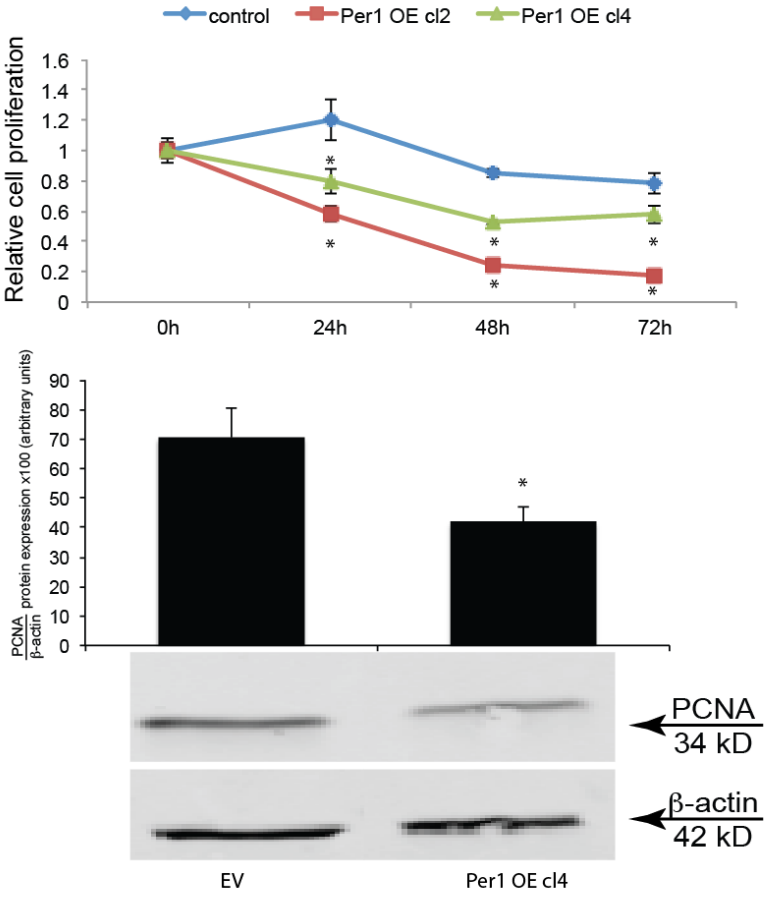

Figure 12 Decreased proliferation in Per1-overexpressing clones. To further confirm that proliferation was inhibited after overexpressing Per1, we performed an MTS assay, which showed decreased proliferation in both overexpressing clones at 24, 48 and 72 hours after 24 hours of serum starvation. Protein levels of PCNA are also shown to be diminished in Per1 OE clone 4. A representative blot is shown at the bottom. Experiments for MTS are mean ± SEM of 3 repeated experiments. Quantification of blots is the mean ± SEM of 4 repeated experiments. *$p < 0.05$ vs. EV. EV=empty vector, Per1 OE cl =Per1 overexpressing clones.

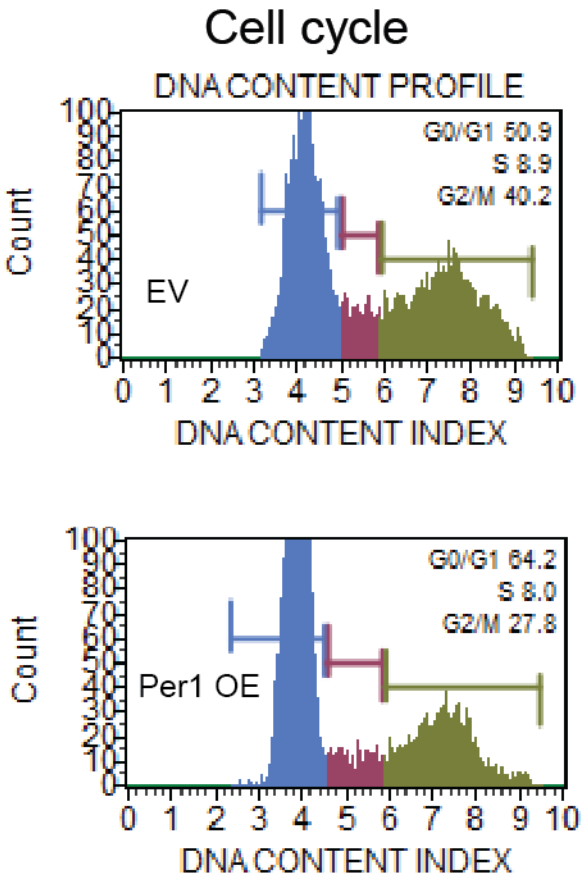

	G0-G1	S	G2/M
EV	50.9%	8.9%	40.2%
Per1 OE cl4	64.2%	8%	27.8%

Figure 13 Decreased number of cells in S phase and G2/M phase in Per1-overexpressing Mz-ChA-1 cells. Cells were serum starved for 24 hours and then put back into complete medium for 24 hours before evaluating the cell cycle. Cell counts and data plots are shown in the top panel and percentage of cells in each cell cycle phase is shown on the bottom. The percentage of cells increased in G0/G1 phase and decreased in S and G2/M phases in Per1-overexpressing cells, indicating that the proliferation rate was diminished after overexpressing Per1. EV = empty vector, Per1 OE = Per1 overexpression.

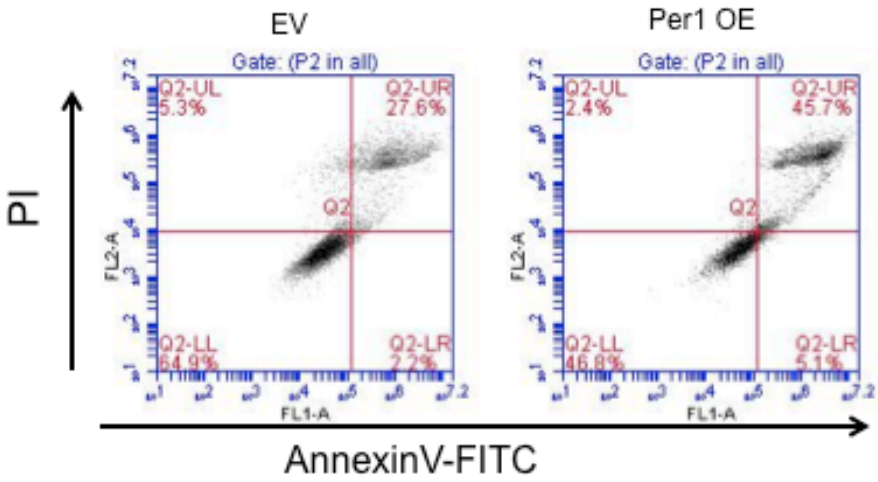

	live cells	early apoptosis	late apoptosis	dead cells
EV	64.9%	2.2%	27.6%	5.3%
Per1 OE	46.8%	5.1%	45.7%	2.4%

Figure 14 Enhanced apoptosis after overexpressing Per1 in Mz-ChA-1 cells. Cell apoptosis was investigated in control and Per1-overexpressing stably transfected cell lines. Cells were stained using an AnnexinV-FITC apoptosis kit and then analyzed using flow cytometry. The gate was set using three controls: unstained, and staining the FITC only and PI only. The data are from double staining of PI and AnnexinV-FITC. By overexpressing the Per1, the percentage of early and late apoptotic cells was largely increased and the percentage of live cells was decreased. Top panel: FACS plots; Bottom panel: Percentage of cells in each apoptosis stage. EV = empty vector; Per1 OE = Per1 overexpression.

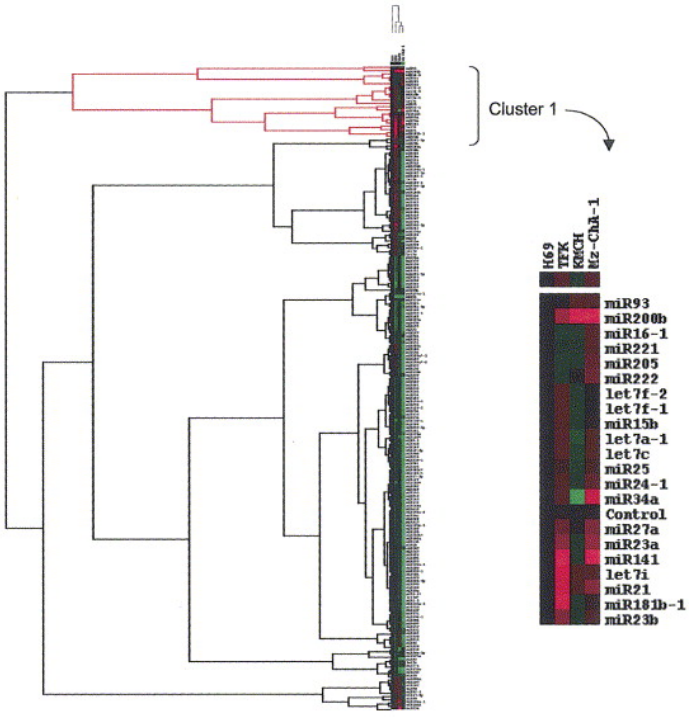

Figure 15 Comparison of miRNA obtained from H69 non malignant cholangiocytes and the human cholangiocarcinoma cell lines Mz-ChA-1 and TFK-1. A heatmap was generated from the average of normalized log-transformed fluorescent intensity for each data set (n=4 separate arrays, each with two probes for each miRNA). A cluster of miRNAs that was upregulated is enlarged and shown in the right panel.

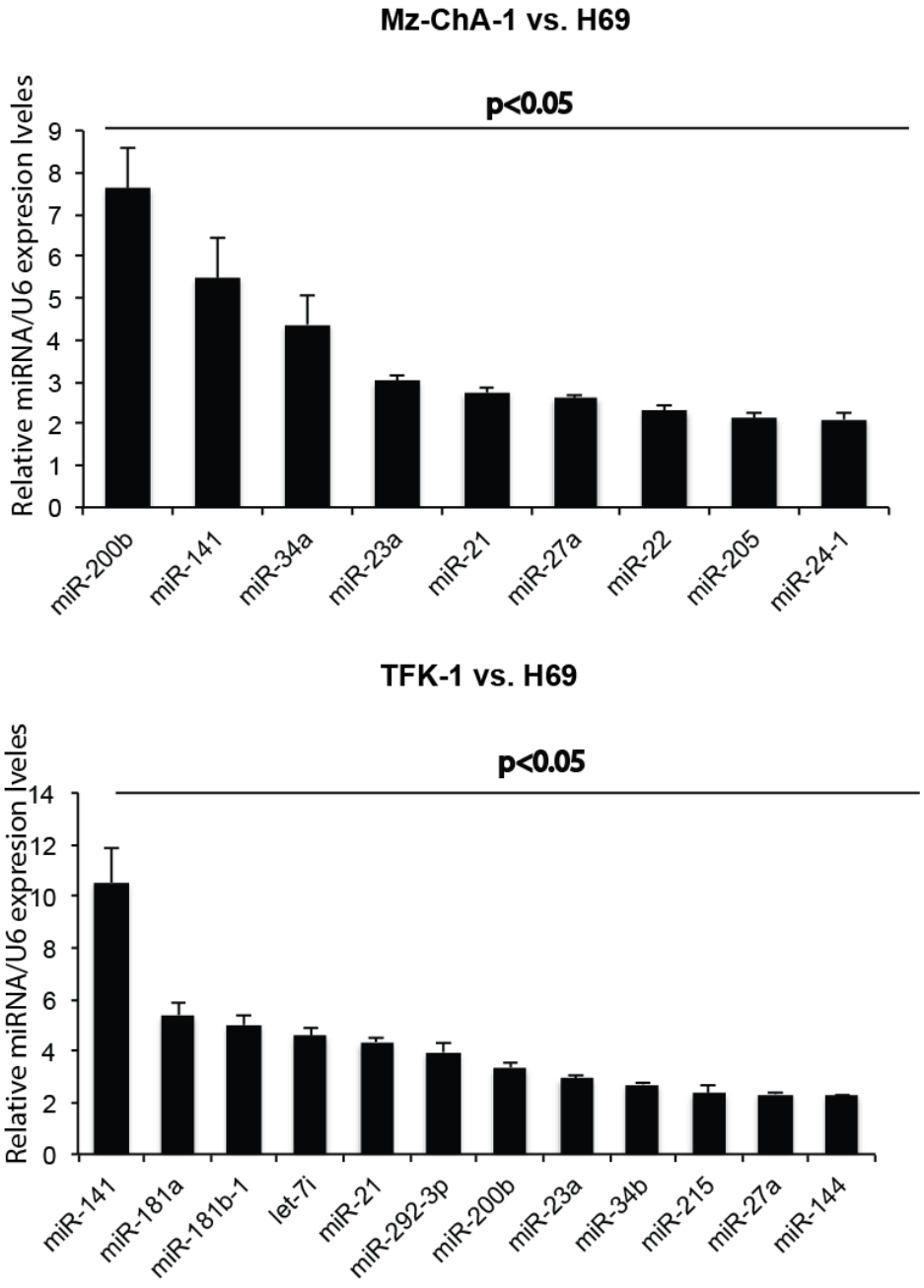

Figure 16 A group of miRNAs with increased expression in CCA cell lines. Expression fold change of upregulated miRNAs was shown in Mz-ChA-1 (upper panel) and TFK-1 (lower panel) cells vs. H69 cells. Data are expressed as mean ± SEM from four experiments of each cell line.

Screening candidate miRNAs that target Per1 in CCA cell lines

As we have shown earlier, Per1 expression was decreased and its circadian rhythm was lost in all CCA cells. By restoration of Per1 expression, CCA cell growth was inhibited. However, no information is known about the upstream regulation of Per1. Here, we hypothesized that dysregulated microRNA may lead to the decreased expression of Per1. We screened the potential miRNAs of Per1 with three target prediction programs that used different algorithms: DIANA-MicroT, Miranda and RNAhybid.

By using DIANA-MicroT V3.0, 22 miRNAs were found that could target hPer1 (Table 2); while 49 miRNAs were found that could possibly target hPer1 as predicted in Miranda (Table 3). When comparing these two miRNA lists, we found that miR-34a, miR-185 and miR-29b were predicted in both DIANA and Miranda. Then we analyzed the free energy and binding sites for miR-34a, miR-185 and miR-29b with Per1 via RNAhybrid. One binding site was found (the same site of prediction as DIANA-MicroT and Miranda) for miR-34a. Besides miR-34a, we also identified one binding site for miR-185 and miR-29b as well (Figure 17). On the other hand, as we showed above, by PCR array analysis, we found a group of microRNAs that were upregulated in Mz-ChA-1 cells. However, miR-34a is the only one that was upregulated in Mz-ChA-1 cells compared with H69 cells, whereas miR-29b and miR-185 showed no significant change in Mz-ChA-1 cells in the microRNA array data (Figure 16). We further examined the expression of miR-34a in Mz-ChA-1 by taqman real-time PCR, which showed

miR-34a increased about four times in Mz-ChA-1 compared with H69, which is consistent with the microRNA array data (Figure 18).

24-hours circadian profile for miR-34a in CCA cells and H69

Since Per1 is a primary output rhythmical gene, we also determined whether the 24-hours expression of miR-34a showed circadian rhythm similar to Per 1. Interestingly, miR-34a displayed rhythmical expression in CCA cells with higher amplitude during the 24-hours period (Figure 19). In H69 cells (normal culture condition), the expression upper peaks for miR-34a were seen at 6 and 18 hours; while the lower peaks showed at 14 and 22 hours. Per1 expression, on the other hand, showed the upper peaks at 2 and 14 hours and lower peaks at 6 and 22 hours. It is worthy to note that Per1 and miR-34a displayed exactly opposite patterns at 6 hours and 14 hours with regard to the upper and lower peaks, indicating the opposite correlation between miR-34a and Per1. In Mz-ChA-1 cells, expression of miR-34a showed shifted phase, higher amplitude and higher expression at all time points compared with H69 cells. In TFK-1 cells, the overall amplitude was not altered very much, however, the period was significantly shortened and the expression level was much higher compared with H69 cells. For HuCC-T1 cells, the overall expression level of miR-34a did not change significantly, however, the amplitude diminished and the circadian rhythm was lost compared with H69 cells (Figure 19).

Table 2 List of miRNAs to target Per1 predicted by DIANA-MicroT

Rank	miRNA name	miTG score
1	hsa-miR-646	15.37
2	hsa-miR-637	13
3	hsa-miR-29a	12.68
4	hsa-miR-29c	12.49
5	hsa-miR-29b	12.48
6	hsa-miR-532-3p	11
7	hsa-miR-485-5p	11
8	hsa-miR-185	11
9	hsa-miR-138	10.81
10	hsa-miR-765	10
11	hsa-miR-484	10
12	hsa-miR-24	9.96
13	hsa-miR-604	9
14	hsa-miR-188-3p	9
15	hsa-miR-497	8.94
16	hsa-miR-424	8.51
17	hsa-miR-939	8
18	hsa-miR-766	8
19	hsa-miR-608	8
20	hsa-miR-149	8
21	hsa-miR-34	7.69
22	hsa-miR-449b	7.68

Table 3 List of miRNAs to target Per1 predicted by Mianda

Rfam ID	Score	Rfam ID2	Score
hsa-miR-222	18.1869	hsa-miR-24	16.0866
hsa-miR-614	18.118	hsa-miR-541*	16.0807
hsa-miR-423-5p	18.0126	hsa-miR-326	16.0366
hsa-miR-138	17.9073	hsa-miR-218-2*	15.9807
hsa-miR-185*	17.7799	hsa-miR-374b*	15.9807
hsa-miR-30c-1*	17.7799	hsa-miR-519a	15.9807
hsa-miR-604	17.6301	hsa-miR-519b-3p	15.9807
hsa-miR-661	17.6176	hsa-miR-514	15.9534
hsa-miR-432	17.5913	hsa-miR-338-3p	15.8749
hsa-miR-769-3p	17.3806	hsa-miR-34a	15.8749
hsa-miR-645	17.3076	hsa-miR-624*	15.8749
hsa-miR-331-3p	17.1234	hsa-miR-221	15.6952
hsa-miR-620	17.1058	hsa-miR-519c-3p	15.6632
hsa-miR-30b*	16.8274	hsa-miR-515-5p	15.6252
hsa-miR-601	16.8274	hsa-miR-657	15.5899
hsa-miR-10b*	16.6157	hsa-miR-626	15.5876
hsa-miR-484	16.6157	hsa-miR-361-5p	15.5574
hsa-miR-145*	16.4041	hsa-miR-640	15.528
hsa-miR-148b*	16.4041	hsa-miR-29b	15.4845
hsa-miR-486-3p	16.3789	hsa-miR-145*	15.3457
hsa-miR-30c-1*	16.2982	hsa-miR-490-5p	15.1814
hsa-miR-484	16.2982	hsa-miR-371-3p	15.0632
hsa-miR-570	16.2982	hsa-miR-889	14.8899
hsa-miR-196b	16.1924	hsa-miR-299-5p	14.7107
hsa-miR-519e*	16.1924		

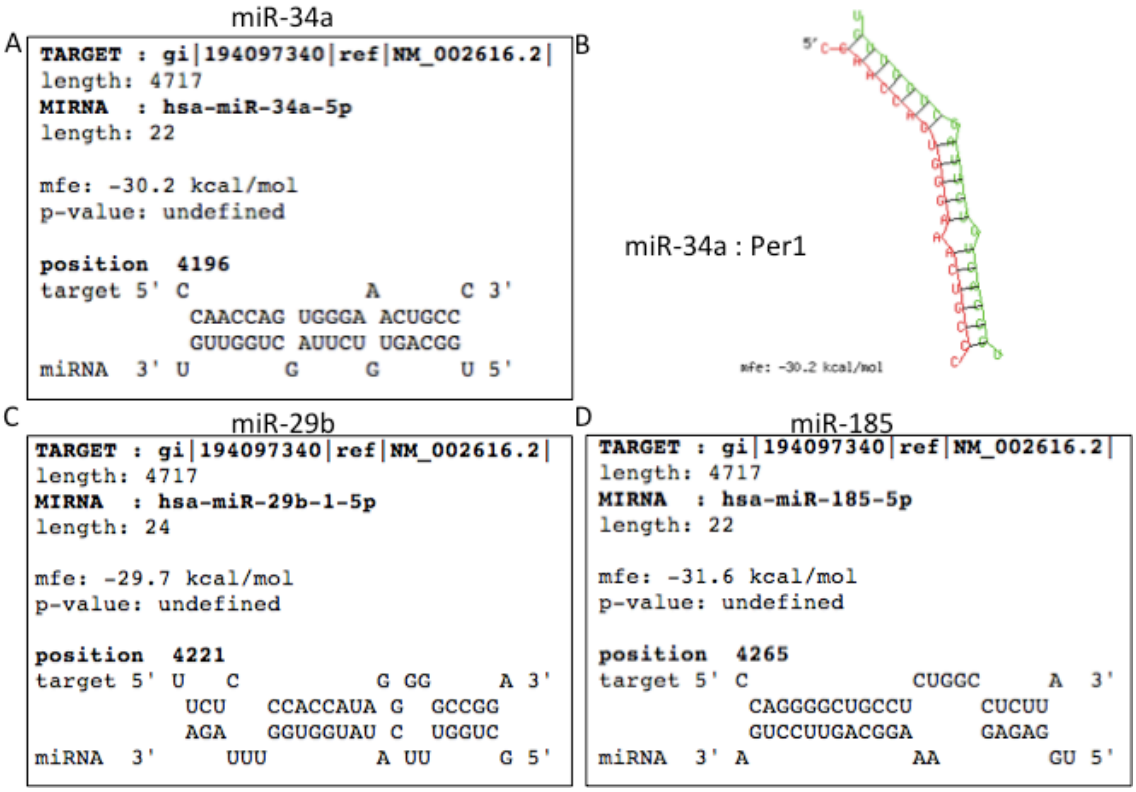

Figure 17 RNA hybridization prediction showed the binding sites of three candidate miRNAs and mRNA of Per1. [A] Schematic picture of the binding site for miR-34a and Per1 indicating the position, minimum free energy; [B] Plot picture for the binding loop that formed between miR-34a and Per1; [C] and [D] Schematic picture of the binding site for miR-29b and miR-185 and Per1 indicating the position, minimum free energy.

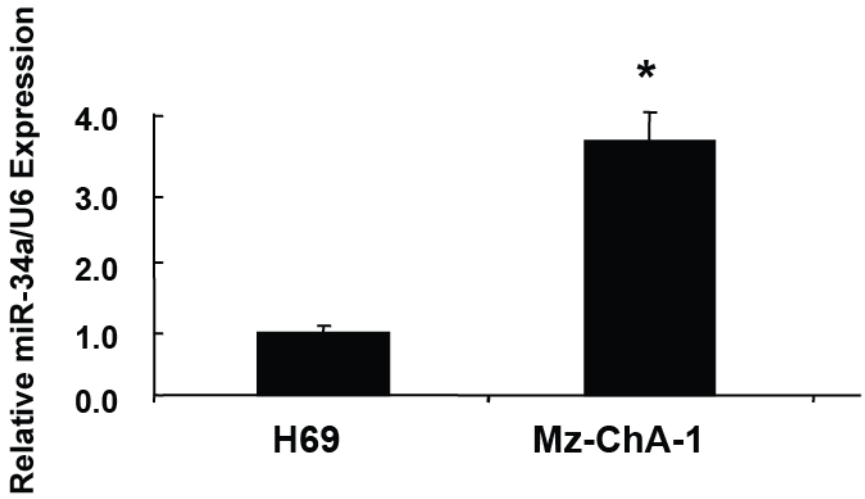

Figure 18 miR-34a expression in H69 and Mz-ChA-1 cells. The expression level of miR-34a was measured in Mz-ChA-1 and H69 cells with Taqman miRNA PCR assay. The data represent the mean ± SEM for 3 experiments. *$p < 0.05$ vs. H69.

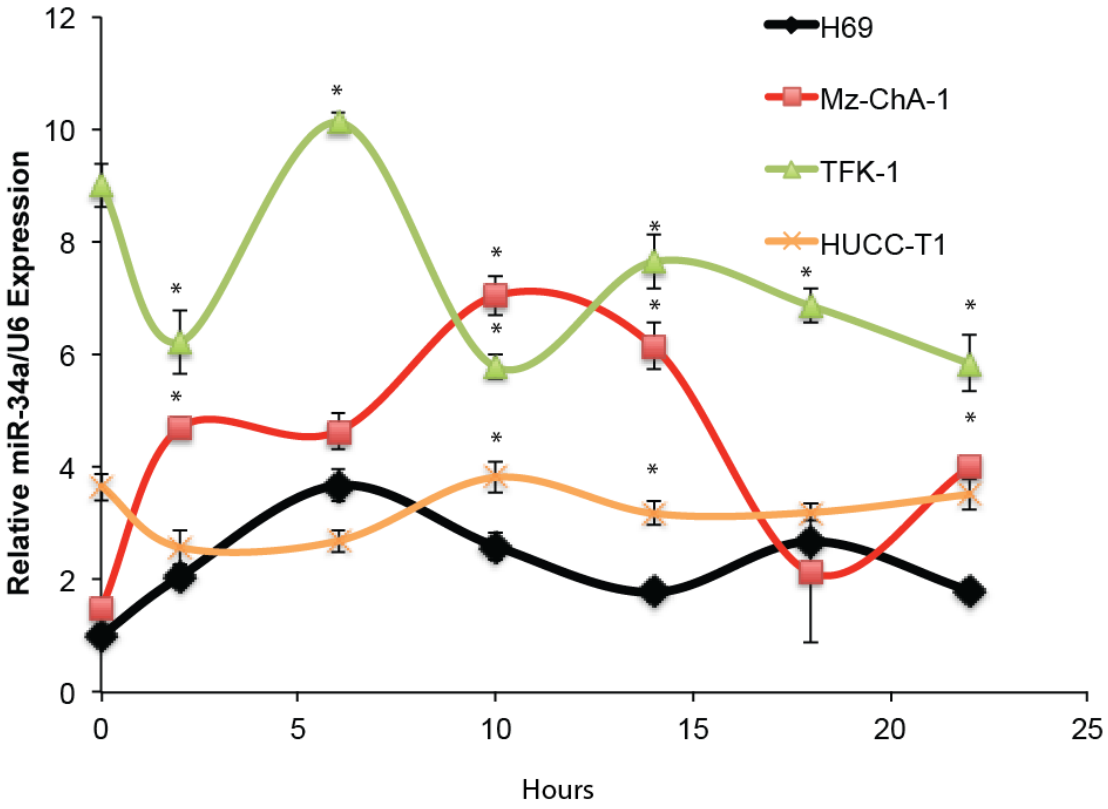

Figure 19 The 24-hours circadian rhythm of miR-34a expression levels in CCA and H69 cell lines. The expression level of miR-34a was measured in extra-hepatic CCA cell lines (Mz-ChA-1 and TFK-1), intra-hepatic CCA cell lines (HUCC-T1) and H69 cells. The cells were stimulated with 50% serum for 2 hours after being serum starved for 48 hours. Samples were taken every four hours until 24 hours. The points represent the mean ± SEM for 3 experiments. *$p <$ 0.05 vs. H69 corresponding time points.

miR-34a was verified as the upstream modulator of Per1

To substantiate that miR-34a directly targets Per1; we generated a luciferase reporter assay with the 3'UTR, which contains potential miR-34a binding sites (pMIR-Per1-WT), or the mutations (pMIR-Per1-mut) inserted in the multiple cloning site (MCS). As shown in Figure 20, when transfecting with miR-34a alone, or pMIR-Per1-WT alone, we did not detect any luciferase activity. Likewise, when co-transfecting miR-34a with pMIR-Per1-mut or control microRNA with pMIR-Per1-WT luciferase activity did not change. Co-transfecting the miR-34a with pMIR-Per1-WT significantly suppressed the luciferase activity, indicating the suppression effect is specific to the 3'-UTR regions and the binding sites are essential for the inhibitory effect of miR-34a on Per1.

Inhibition of miR-34a expression diminished CCA proliferation and invasion

Since we have shown that Per1 overexpression inhibited tumor growth and promoted apoptosis by regulating the cell cycle, we proposed to study whether inhibition of miR-34a could affect the proliferation and invasion in CCA cells, thus regulating Per1 expression. To evaluate the roles of miR-34a in the regulation of CCA growth *in vitro*, we transiently transfected the miR-34a inhibitor and relative control in Mz-ChA-1, TFK-1, HUCC-T1 and H69 cell lines. As shown in Figure 21, after inhibition of miR-34a expression, the proliferation of Mz-ChA-1 cells was significantly inhibited at 24, 48 and 72 hours; whereas the

```
    3' .UGUUGGU.CGAUUCUGUGACGGU 5'  Human miRNA: hsa-miR-34a (UCSC) (Rfam)
         |||||| | |::|| ||||||      Score: 158, Energy: -26.5 kCal/mol
85:5' -CCAACCA.G-UGGGAAACUGCCC 3'  Human transcript: Period circadian protein 1
       |||||||   | ||||||||||      Conservation: 95.0%
88:5' ACCAACCA-A.UAGGAAACUGCCC 3'  Mouse transcript: Period circadian protein 1
       | ||||||   ||:|| ||||||      Score: 154, Energy: -23.1 kCal/mol
    3' UUGUUGGUCG.AUUCUGUGACGGU 5'  Mouse miRNA: mmu-miR-34a (Rfam)
```

A

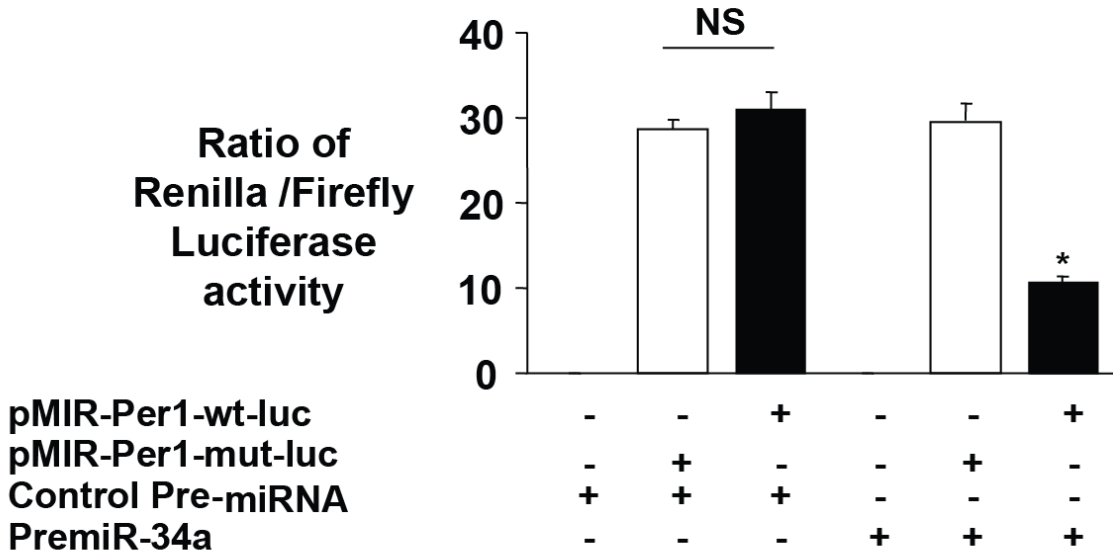

B

Figure 20 Per1 was predicted and verified as a target of miR-34a. [A] Conserved target site of hsa-miR-34a on gene Per1. The potential binding sites are labeled in red color. [B] Mz-ChA-1 cells were transfected with 1μg of a Renilla luciferase expression construct pRL-TK and 1μg of the pMIR-PER1-wt-luc or pMIR-PER1-mut-luc firefly luciferase expression construct, along with either miR-34a precursor or control precursor. Luciferase assays were performed after 48 hours using the dual luciferase reporter assay system. The Renilla luciferase activity was normalized to that of firefly luciferase activity for each sample. A decrease in relative renilla luciferase activity in the presence of miR-34a indicates the presence of a miR-34a-modulated target sequence in the 3'-UTR of PER1. Data represents mean±SEM from eight separate experiments. *p<0.05 relative to controls.

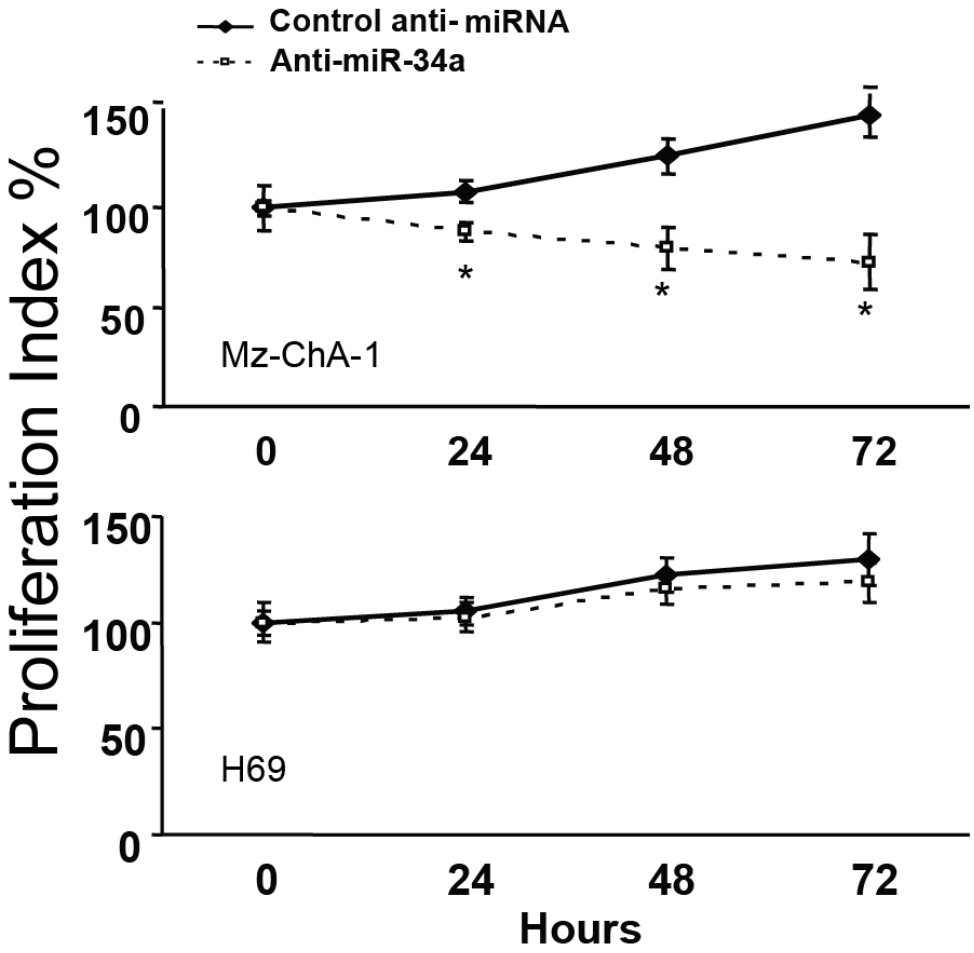

Figure 21 Inhibition of miR-34a decreased the proliferation of CCA cells but not the non-malignant cholangiocytes. Mz-ChA-1 (Top Panel) and H69 (Bottom Panel) cells (5 x 10^4cells/well) in 96-well plates were transfected with either anti-miRNA inhibitor for miR-34a or with its respective control inhibitor. Cell proliferation was assessed after 72 hours using a viable cell assay. Transfection of Mz-ChA-1 with inhibitor to miR-34a decreased proliferation to 71.7 ± 12.6 % of control after 72 hours. Cell growth was not significantly altered in H69 cells transfected with miR-34a inhibitor after 72 hours (97.5 ± 11.0 % of control). The mean ± SEM from four separate experiments are illustrated.

proliferation of H69 did not show significant change after inhibiting the miR-34a expression.

Furthermore, the invasion ability was also examined after inhibiting the expression of miR-34a. As shown in Figure 22, the ability to invade was significantly decreased in CCA cell lines compared to vector-transfected cells. However, H69 cells did not show any difference after transfection with the miR-34a inhibitor. Taken together, these data indicate that miR-34a acts as an onco-miR that can promote proliferation and invasion in CCA cells.

We have previously shown that Per1 overexpression could enhance apoptosis. Bcl-2 is considered to be an anti-apoptotic protein and is thus classified as an oncogene during tumorigenesis (133). Here, we found the expression of Per1 is decreased and expression of bcl-2 is increased after the inhibition of miR-34a, indicating that miR-34a could promote tumorigenesis at least partly through inhibition of apoptosis (Figure 23).

Prolonged dark exposure of CCA xenograft did not change the tumor growth in *in vivo* models

In order to evaluate the relationship between central circadian system and the local circadian system, we exposed nude mice (in which we injected with Mz-ChA-1 cells) to complete dark or a 12:12 dark: light cycle (control) before measuring tumor growth. In control group, the tumors all grew to a similar size,

as shown in the left panel of Figure 24; whereas, the tumors in animals that were exposed to the dark for 42 days showed a significant difference between different flanks of the same mice and between the different mice from the same group (right panel of Figure 24). However, when looking at the overall average tumor growth rate between the control and dark groups, the tumor volume did not show a significant difference (Figure 25).

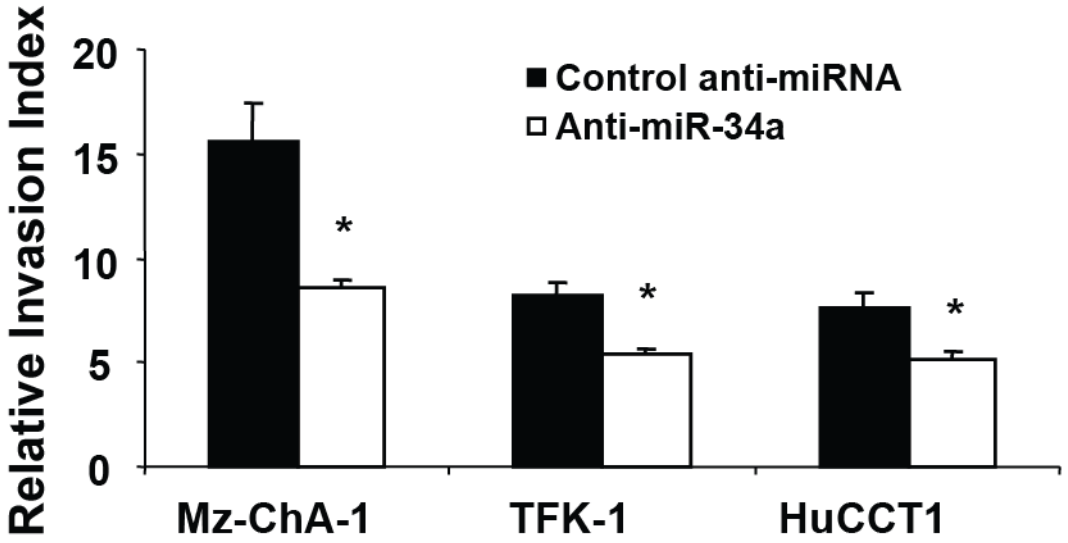

Figure 22 Effect of miR-34a inhibitor on invasion in CCA cells. To assess the effect of miR-34a on tumor spread, Mz-ChA-1, TFK and HuCCT1 cells were transfected with either control or anti-miR-34a inhibitor. Anti-miR-34a decreased cell invasion in all three CCA cell lines studied compared to controls. These results support a functional role for miR-34a in mediating cell invasion in malignant cholangiocytes, and provide a mechanism by which over-expression of miR-34a may contribute to tumor spread. * $p < 0.05$ when compared to control miRNA inhibitors.

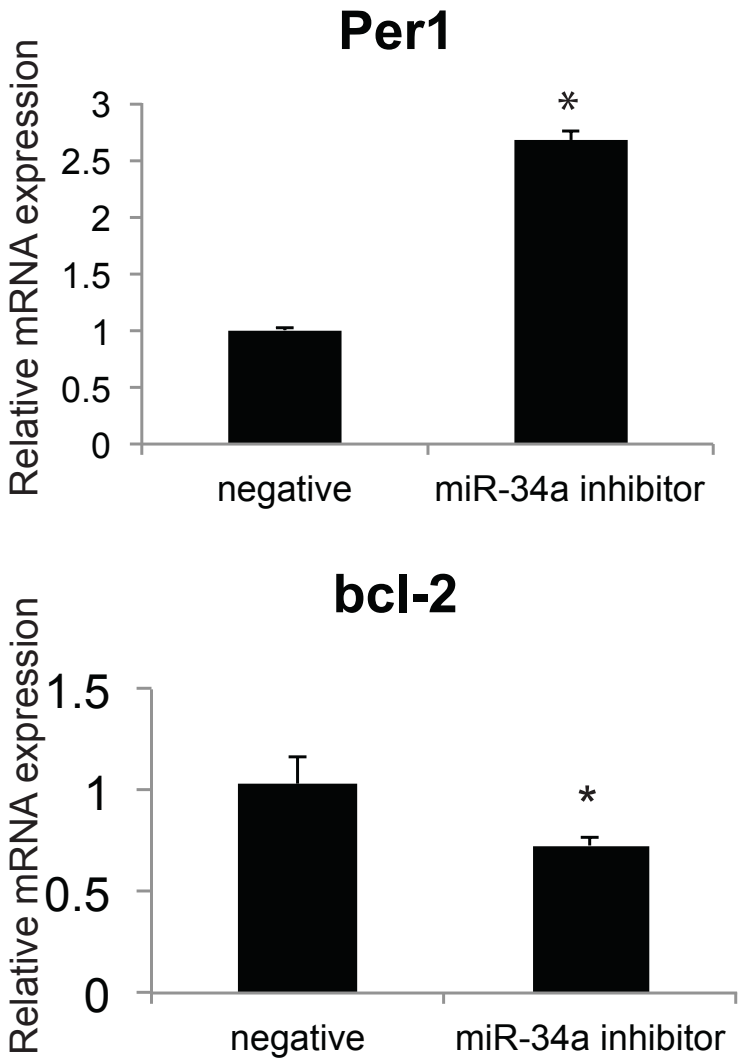

Figure 23 Inhibition of miR-34a stimulates the expression of Per1 and inhibits the expression of bcl-2. Mz-ChA-1 cells in 6-well plates were transfected with either anti-miRNA inhibitor to miR-34a or with its respective control inhibitor (negative) for 48 hours. Total mRNA was harvested and expression of Per1 and anti-apoptotic factor was measured by real-time PCR. Data represents mean ± SEM from eight separate experiments. *p<0.05 relative to controls.

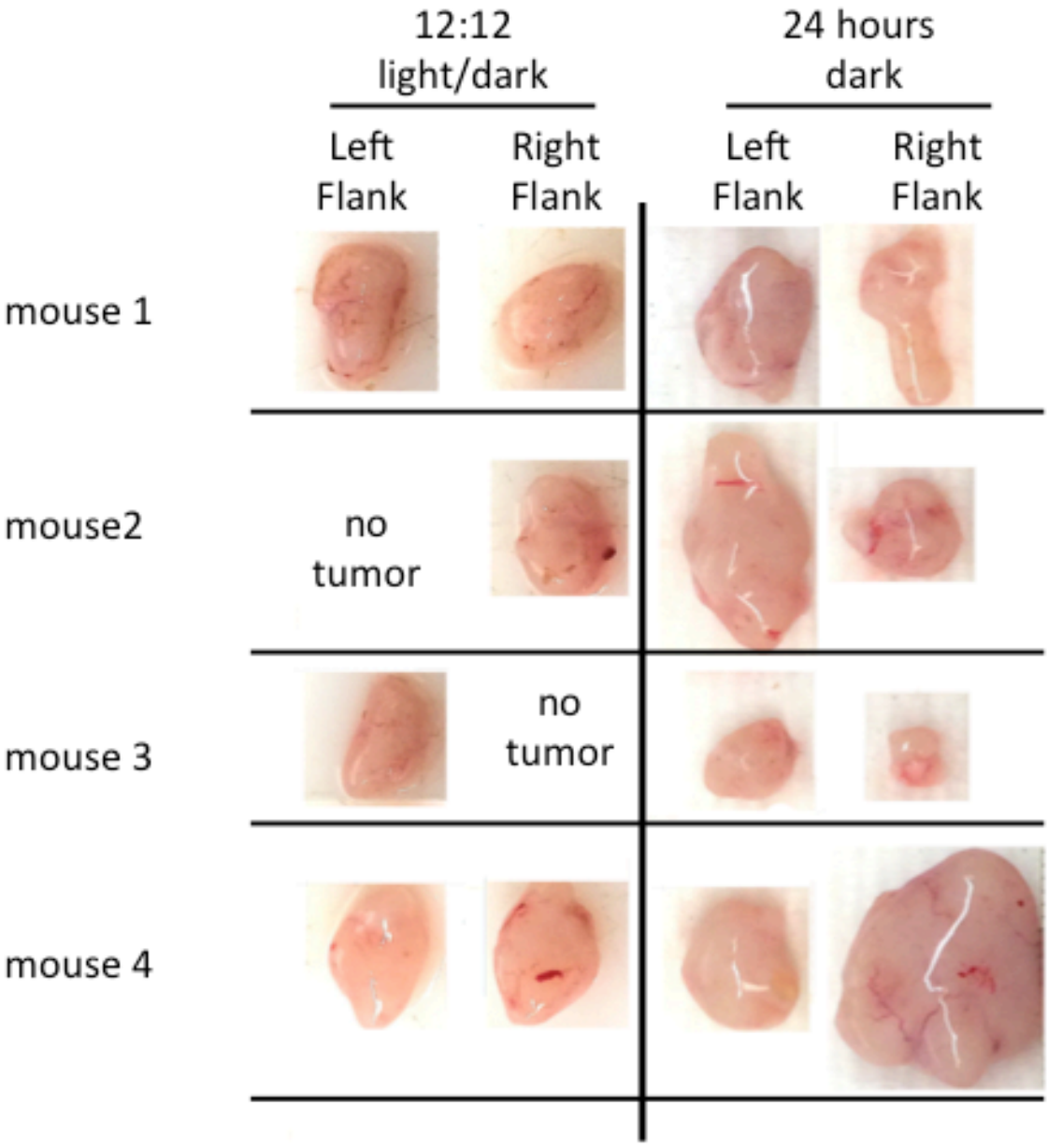

Figure 24 CCA tumors dispalyed size variation in the dark group but not in the control group. Male BALB/c nude (nu/nu) mice bearing CCA xenografts were kept in a 12-h light-dark cycle or a 24-hours continuously dark cycle. After 42 days, mice were sacrificed and the pictures of each tumor were obtained.

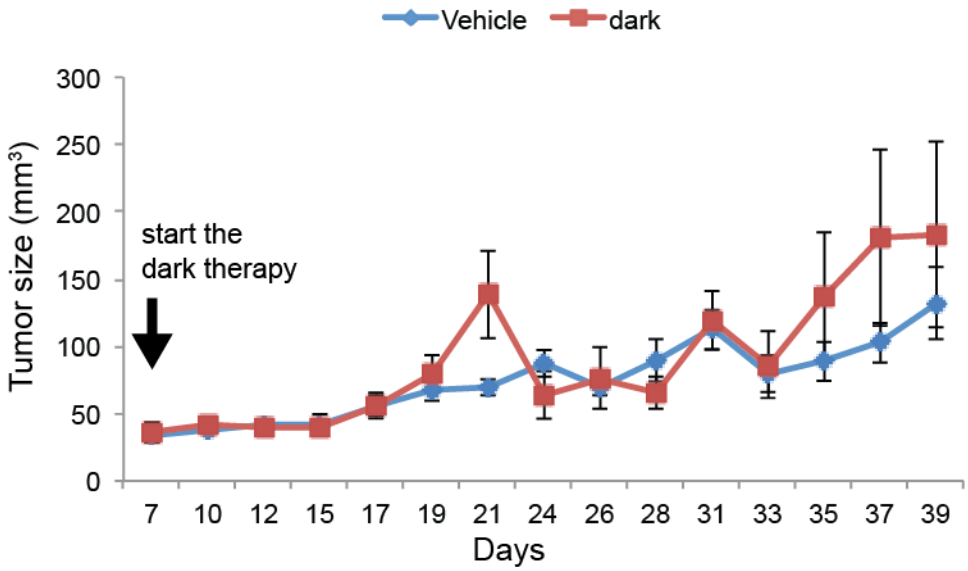

Figure 25 No significant difference in tumor volume was observed between control and dark groups. Mz-ChA-1 cells ($5x10^6$) were suspended in 0.25 mL of extracellular matrix gel and injected in the back flank of nude mice. After the tumor was established, mice were randomly divided into two groups: normal 12-hour light-dark cycles and 24-hours continuously dark group. Tumor growth was measured three times a week by an electronic caliper, and volume was determined as follows: tumor volume (mm^3) = 0.5 × length (mm) × width (mm) × height (mm). Data are mean ± SEM of tumor size evaluations from four mice per each group of animals.

CHAPTER IV

SUMMARY AND CONCLUSION

In our study, we found that the expression of core clock genes Per1/2/3, Bmal1, clock and cry1/2 was dysregulated in both intra- and extra-hepatic cell lines as compared with H69 cells. The immunoreactivity of Bmal1 was increased in human CCA biopsies. Furthermore, we demonstrated that the rhythmic expression of core clock genes, including Bmal1, CLOCK, Cry1/2 and Per1/2/3, was disrupted in all or some of the CCA cell lines compared with H69 cells. Specifically, expression of Per1 was largely decreased in all six CCA cell lines we examined and the human CCA biopsies. The 24-hours profile of mRNA expression of Per1 showed loss of circadian rhythm in all CCA cell lines. Furthermore, the CCGs WEE1 and DBP also lost 24-hours circadian expression in Mz-ChA-1 cells compared with H69 cells. Restoration of Per1 inhibited the proliferation, promoted the apoptosis and decreased the percentage of cells in the G2/M phase and S phase of the cell cycle. Then, miR-34a, miR-29b and miR-185 was predicted by three different software programs to target Per1. Also, miR-34a was verified to target Per1 by luciferase reporter assay. Inhibition of miR-34a could inhibit the proliferation and invasion of Mz-ChA-1, TFK-1 and HuCC-T1 cells. Finally, we also performed an *in vivo* study and were able to show that disruption of central circadian system by exposing the nude mice to continuous darkness would not affect the average tumor growth.

In our study, we first demonstrated that the circadian rhythm of core clock genes in non-malignant cholangiocytes, and then showed this rhythm was disrupted in CCA. Consistent with our research, disruption of circadian rhythms was found in both human and animal models of tumors (78). Circadian disruption was found to increase susceptibility to cancer development in all essential organs in humans, leading to breast, hepatocellular carcinoma, ovarian, lung, pancreatic, prostate, acute myeloid leukemia, osteosarcoma, colorectal, and endometrial cancer (52, 53, 134-140). Indeed, circadian rhythm is proposed as an independent cancer risk factor for humans(135). Disrupted circadian rhythm not only happens in cancer development, but also happens in other disorders such as obesity, type 2 diabetes and insulin resistance (141, 142). Clock mutant mice fed a high fat diet showed significantly higher triglyceride content in the liver (143). Bmal1 knockout mice showed hepatic steatosis with regular diet feeding (144). All of these findings indicate that disruption of circadian homeostasis would lead to pathophysiological changes in all essential organs.

It has been previously reported that Per1, one of the output primary clock genes, can act as a tumor suppressor gene in various tumors. Decreased Per1 expression was found in colon cancer, which correlated with estrogen receptor-beta expression via epigenetic regulation (145). Among 35 endometrial carcinomas and paired non-tumor tissues, Per1 expression was significantly decreased and accompanied with hyper-methylation in the CpG area of the

promoter region of Per1 (146). Similar deregulation of Per1 was also found in breast cancer, non-small cell lung cancer, pancreatic, HCC and prostate cancer (72, 147-149). Likewise, we found that Per1 expression was decreased in both intra- and extra- hepatic cell lines. Further investigation needs to be done to examine whether the epigenetic modification is involved in the decreased expression of Per1.

By overexpressing Per1, we found that tumor growth of CCA is inhibited via inhibition of proliferation and enhanced apoptosis. Indeed, Per1 has been found to regulate cell growth by regulating the cell cycle (150). When the Per1 expression reached a high level, the percentage of cells that enter into the M phase is reduced. The potential mechanisms could be explained by the finding that Per1 protein interacts with the checkpoint protein ataxia telangiectasia mutated (ATM) and the checkpoint kinase 2 (CHK2), leading to DNA repair and cell cycle arrest and/or apoptosis (132). However, the inhibition of Per1 in non-malignant cholangiocytes should be also investigated in the future to further validate whether Per1 has a rate-limiting role in the malignant transformation of cholangiocytes.

One question may rise regarding how disrupted clock genes could lead to the malignant transformation of cholangiocytes. Previous findings indicate that the core clock gene machinery could regulate a group of genes named clock-controlled genes (CCGs) (56). Hundreds of protein-coding genes showed a 24-hours oscillation expression pattern in liver (151). The expression of CCGs might

shed light on this complicated question. In our study, we found previously reported CCGs, WEE1 and DBP, lost circadian rhythms in CCA cell lines. WEE1 is a nuclear kinase that could inhibit Cdk1 by phosphorylating it on two different sites (150). The regulation of Cdk1 by WEE1 is important in controlling the G2/M checkpoint (132). This is interesting because after we restored Per1 expression, the percentage of cells in the G2/M phase was decreased in Mz-ChA-1 cells, indicating that Per1 might directly regulate expression of WEE1, which affects the downstream cell cycle-related molecules.

It is interesting that we found not only do CCGs show circadian rhythm, but miRNAs that regulate Per1 expression also show circadian rhythm. We found that miR-34a displayed ultracircadian rhythm in CCA cells and normal circadian rhythm in H69 cells. The high peak levels of miR-34a coincided with the lowest level of Per1 expression, suggesting the direct modulation of Per1 expression by miR-34a. This phenomenon actually has been predicted by a computational model for the interaction of core clock genes with microRNAs, which indicated that miRNA-mediated regulation of clock genes could enhance the robustness of the circadian rhythms(152). The circadian rhythm exists not only in miR-34a expression in cholangiocytes. For example, miR-122, as a hepatocyte-specific miRNA, also has circadian rhythm in mouse liver (94). The rhythmic transcription of miR-122 precursors has been demonstrated by northern blots. By genetic loss of function and gain-of-function experiments, the orphan nuclear receptor REV-ERBα has been identified as the major regulator

of miR-122. All these findings together indicate that the miRNAs and clock genes could interact with each other in a 24-hours oscillation fashion to fine-tune the circadian rhythm. Further study needs to be performed regarding the events upstream of miR-34a and whether the miR-34a is regulated at the transcriptional level.

As previously shown the circadian rhythm of core clock genes was not completely lost in malignant cells. They displayed ultracircadian rhythms with a shorter period in murine tumor models (reviewed in (153)). We also found that the circadian rhythm of some core clock genes still exists in some of the CCA cells. This indicates that the effects of some of the core clock genes might not be essential during the malignant transformation of cholangiocytes. Further gain-of function and lost-of-function studies need to be performed to further define the role of other clock genes.

Prolonged dark could inhibit biliary hyperplasia and biliary fibrosis by regulating core clock gene expression (154). BDL mice exposed to continuous darkness for one week showed decreased biliary fibrosis and cholangiocyte proliferation due to inhibiting the core clock gene proliferation. We also wanted to see whether the darkness therapy could affect tumor growth in CCA. However, exposure of nude mice to continuous darkness did not significantly inhibit the proliferation of CCA xenografts. However, it is interesting to note that the tumor volume of CCA in normal light/dark cycle displayed consistent and small deviation, whereas the tumor volume of CCA in mice exposed to

continuous darkness showed huge differences between different animals and large deviations. This indicates dark therapy might affect the tumor growth in a different mechanism compared with that in cholestasis. Further studies need to confirm whether circadian rhythms of these core clock genes are changed.

In summary, our work helps to define the role of circadian rhythm of core clock genes in CCA, the correlation of microRNA to clock genes and CCA and the therapeutic effect of Per1 and miR-34a in CCA. Our findings build the bridge of microRNA and circadian rhythm in CCA for the first time. The modulation of Per1 and miR-34a could provide a possible prognostic and therapeutic effect in clinical applications. Further studies need to be performed regarding the role of other core clock genes in CCA as well as the possible involvement of other miRNAs. The potential molecular mechanism(s) of how Per1, miR-34a and the upstream regulator lead to the malignant transformation of cholangiocytes also needs to be further investigated.

NOMENCLATURE

CCA	Cholangiocarcinoma
PSC	Primary Sclerosing Cholangitis
cAMP	3’-5’-cyclic adenosine monophosphate
PKA	protein kinase A
PKC	protein kinase C
CFTR	cystic fibrosis transmembrane conductance regulator
AE2	Cl-/HCO3- anion exchanger 2
SCN	suprachiasmatic nucleus
CLOCK	circadian locomotor output cycles kaput
Bmal1	brain and muscle-Arntlike1
Per1/2/3	Period 1, 2, and 3
Cry1/2	cryptochrome 1 and 2
CCGs	clock-controlled genes
RISC	RNA-induced silencing complex
PDCD4	programmed cell death 4
CREM	cAMP responsive element modulator
FACS	fluorescence-activated cell sorting
PI	propidium iodide
FITC	fluorescein isothiocyanate
EV	empty vector

OE	overexpressing
PCNA	proliferating cell nuclear antigen
PCR	polymerase chain reaction

REFERENCES

1. Alpini G, RT P, LaRusso NF: The pathobiology of biliary epithelia. In: Arias I, Boyer JL, Chrisari F, Fausto N, Schachter D, Shafritz D, eds. The Liver: Biology & Pathobiology. 4th ed. Philadephia, PA: Lippincott Williams & Wilkins, 2001; 421-435.

2. Alpini G, Roberts S, Kuntz SM, Ueno Y, Gubba S, Podila PV, LeSage G, et al. Morphological, molecular, and functional heterogeneity of cholangiocytes from normal rat liver. Gastroenterology 1996;110:1636-1643.

3. Alpini G, Lenzi R, Sarkozi L, Tavoloni N. Biliary physiology in rats with bile ductular cell hyperplasia. Evidence for a secretory function of proliferated bile ductules. J Clin Invest 1988;81:569-578.

4. Kanno N, LeSage G, Glaser S, Alpini G. Regulation of cholangiocyte bicarbonate secretion. Am J Physiol Gastrointest Liver Physiol 2001;281:G612-625.

5. Xia X, Francis H, Glaser S, Alpini G, LeSage G. Bile acid interactions with cholangiocytes. World J Gastroenterol 2006;12:3553-3563.

6. Han Y, Glaser S, Meng F, Francis H, Marzioni M, McDaniel K, Alvaro D, et al. Recent advances in the morphological and functional heterogeneity of the biliary epithelium. Exp Biol Med (Maywood) 2013;238:549-565.

7. Kanno N, LeSage G, Glaser S, Alvaro D, Alpini G. Functional heterogeneity of the intrahepatic biliary epithelium. Hepatology 2000;31:555-561.

8. LeSage G, Benedetti A, Glaser S, Marucci L, Tretjak Z, Caligiuri A, Rodgers R, et al. Acute carbon tetrachloride feeding selectively damages large, but not small, cholangiocytes from normal rat liver. Hepatology 1999;29:307-319.

9. LeSage G, Glaser S, Marucci L, Benedetti A, Phinizy JL, Rodgers R, Caligiuri A, et al. Acute carbon tetrachloride feeding induces damage of large but not small cholangiocytes from BDL rat liver. Am J Physiol Gastrointest Liver Physiol 1999;276:G1289-1301.

10. Alpini G, Glaser S, Robertson W, Rodgers RE, Phinizy JL, Lasater J, LeSage G. Large but not small intrahepatic bile ducts are involved in secretin-regulated ductal bile secretion. Am J Physiol Gastrointest Liver Physiol 1997;272:G1064-1074.

11. Francis H, Franchitto A, Ueno Y, Glaser S, DeMorrow S, Venter J, Gaudio E, et al. H3 histamine receptor agonist inhibits biliary growth of BDL rats by downregulation of the cAMP-dependent PKA/ERK1/2/ELK-1 pathway. Lab Invest 2007;87:473-487.

12. Alpini G, Ulrich CD, 2nd, Phillips JO, Pham LD, Miller LJ, LaRusso NF. Upregulation of secretin receptor gene expression in rat cholangiocytes after bile duct ligation. Am J Physiol Gastrointest Liver Physiol 1994;266:G922-928.

13. Korner M, Hayes GM, Rehmann R, Zimmermann A, Scholz A, Wiedenmann B, Miller LJ, et al. Secretin receptors in the human liver: expression in biliary tract and cholangiocarcinoma, but not in hepatocytes or hepatocellular carcinoma. J Hepatol 2006;45:825-835.

14. Banales JM, Arenas F, Rodriguez-Ortigosa CM, Saez E, Uriarte I, Doctor RB, Prieto J, et al. Bicarbonate-rich choleresis induced by secretin in normal rat is taurocholate-dependent and involves AE2 anion exchanger. Hepatology 2006;43:266-275.

15. Martinez-Anso E, Castillo JE, Diez J, Medina JF, Prieto J. Immunohistochemical detection of chloride/bicarbonate anion exchangers in human liver. Hepatology 1994;19:1400-1406.

16. Fan B, Malato Y, Calvisi DF, Naqvi S, Razumilava N, Ribback S, Gores GJ, et al. Cholangiocarcinomas can originate from hepatocytes in mice. J Clin Invest 2012;122:2911-2915.

17. Holczbauer A, Factor VM, Andersen JB, Marquardt JU, Kleiner DE, Raggi C, Kitade M, et al. Modeling pathogenesis of primary liver cancer in lineage-specific mouse cell types. Gastroenterology 2013;145:221-231.

18. Khan SA, Toledano MB, Taylor-Robinson SD. Epidemiology, risk factors, and pathogenesis of cholangiocarcinoma. HPB (Oxford) 2008;10:77-82.

19. Khan SA, Davidson BR, Goldin RD, Heaton N, Karani J, Pereira SP, Rosenberg WM, et al. Guidelines for the diagnosis and treatment of cholangiocarcinoma: an update. Gut 2012;61:1657-1669.

20. Everhart JE, Ruhl CE. Burden of digestive diseases in the United States Part III: Liver, biliary tract, and pancreas. Gastroenterology 2009;136:1134-1144.

21. Tyson GL, El-Serag HB. Risk factors for cholangiocarcinoma. Hepatology 2011;54:173-184.

22. Shin HR, Oh JK, Lim MK, Shin A, Kong HJ, Jung KW, Won YJ, et al. Descriptive epidemiology of cholangiocarcinoma and clonorchiasis in Korea. J Korean Med Sci 2010;25:1011-1016.

23. Mabrut JY, Bozio G, Hubert C, Gigot JF. Management of congenital bile duct cysts. Dig Surg 2010;27:12-18.

24. Palmer WC, Patel T. Are common factors involved in the pathogenesis of primary liver cancers? A meta-analysis of risk factors for intrahepatic cholangiocarcinoma. J Hepatol 2012;57:69-76.

25. Shaib YH, El-Serag HB, Nooka AK, Thomas M, Brown TD, Patt YZ, Hassan MM. Risk factors for intrahepatic and extrahepatic cholangiocarcinoma: a hospital-based case-control study. Am J Gastroenterol 2007;102:1016-1021.

26. Honjo S, Srivatanakul P, Sriplung H, Kikukawa H, Hanai S, Uchida K, Todoroki T, et al. Genetic and environmental determinants of risk for cholangiocarcinoma via Opisthorchis viverrini in a densely infested area in Nakhon Phanom, northeast Thailand. Int J Cancer 2005;117:854-860.

27. Tannapfel A, Sommerer F, Benicke M, Katalinic A, Uhlmann D, Witzigmann H, Hauss J, et al. Mutations of the BRAF gene in cholangiocarcinoma but not in hepatocellular carcinoma. Gut 2003;52:706-712.

28. Songserm N, Promthet S, Sithithaworn P, Pientong C, Ekalaksananan T, Chopjitt P, Parkin DM. MTHFR polymorphisms and Opisthorchis viverrini infection: a relationship with increased susceptibility to cholangiocarcinoma in Thailand. Asian Pac J Cancer Prev 2011;12:1341-1345.

29. Bartlett D, Ramanathan R, Ben-Josef E: Cancer of the biliary tree. In: DeVita V, Lawrence T, Rosenberg S, eds. DeVita, Hellman, and Rosenberg's Cancer: Principles and Practice of Oncology. Philadelphia, PA: Lippincott Williams & Wilkins, 2011.

30. Rizvi S, Gores GJ. Pathogenesis, diagnosis, and management of cholangiocarcinoma. Gastroenterology 2013;145:1215-1229.

31. Endo I, Gonen M, Yopp AC, Dalal KM, Zhou Q, Klimstra D, D'Angelica M, et al. Intrahepatic cholangiocarcinoma: rising frequency, improved survival, and determinants of outcome after resection. Ann Surg 2008;248:84-96.

32. Choi SB, Kim KS, Choi JY, Park SW, Choi JS, Lee WJ, Chung JB. The prognosis and survival outcome of intrahepatic cholangiocarcinoma following surgical resection: association of lymph node metastasis and lymph node dissection with survival. Ann Surg Oncol 2009;16:3048-3056.

33. Woo SM, Lee WJ, Kim JH, Kim DH, Han SS, Park SJ, Kim TH, et al. Gemcitabine plus cisplatin versus capecitabine plus cisplatin as first-line chemotherapy for advanced biliary tract cancer: a retrospective cohort study. Chemotherapy 2013;59:232-238.

34. Kuhlmann JB, Blum HE. Locoregional therapy for cholangiocarcinoma. Curr Opin Gastroenterol 2013;29:324-328.

35. Kanno N, Lesage G, Phinizy JL, Glaser S, Francis H, Alpini G. Stimulation of alpha2-adrenergic receptor inhibits cholangiocarcinoma growth through modulation of Raf-1 and B-Raf activities. Hepatology 2002;35:1329-1340.

36. Coufal M, Invernizzi P, Gaudio E, Bernuzzi F, Frampton GA, Onori P, Franchitto A, et al. Increased local dopamine secretion has growth-promoting effects in cholangiocarcinoma. Int J Cancer 2010;126:2112-2122.

37. Francis H, Onori P, Gaudio E, Franchitto A, DeMorrow S, Venter J, Kopriva S, et al. H3 histamine receptor-mediated activation of protein kinase Calpha inhibits the growth of cholangiocarcinoma in vitro and in vivo. Mol Cancer Res 2009;7:1704-1713.

38. Meng F, Han Y, Staloch D, Francis T, Stokes A, Francis H. The H4 histamine receptor agonist, clobenpropit, suppresses human cholangiocarcinoma progression by disruption of epithelial mesenchymal transition and tumor metastasis. Hepatology 2011;54:1718-1728.

39. Francis H, DeMorrow S, Venter J, Onori P, White M, Gaudio E, Francis T, et al. Inhibition of histidine decarboxylase ablates the autocrine tumorigenic effects of histamine in human cholangiocarcinoma. Gut 2012;61:753-764.

40. Fava G, Demorrow S, Gaudio E, Franchitto A, Onori P, Carpino G, Glaser S, et al. Endothelin inhibits cholangiocarcinoma growth by a decrease in the vascular endothelial growth factor expression. Liver Int 2009;29:1031-1042.

41. Onori P, DeMorrow S, Gaudio E, Franchitto A, Mancinelli R, Venter J, Kopriva S, et al. Caffeic acid phenethyl ester decreases cholangiocarcinoma growth by inhibition of NF-kappaB and induction of apoptosis. Int J Cancer 2009;125:565-576.

42. DeMorrow S, Francis H, Gaudio E, Venter J, Franchitto A, Kopriva S, Onori P, et al. The endocannabinoid anandamide inhibits cholangiocarcinoma growth via activation of the noncanonical Wnt signaling pathway. Am J Physiol Gastrointest Liver Physiol 2008;295:G1150-1158.

43. Fava G, Marucci L, Glaser S, Francis H, De Morrow S, Benedetti A, Alvaro D, et al. gamma-Aminobutyric acid inhibits cholangiocarcinoma growth by cyclic AMP-dependent regulation of the protein kinase A/extracellular signal-regulated kinase 1/2 pathway. Cancer Res 2005;65:11437-11446.

44. Kanno N, Glaser S, Chowdhury U, Phinizy JL, Baiocchi L, Francis H, LeSage G, et al. Gastrin inhibits cholangiocarcinoma growth through increased apoptosis by activation of Ca2+-dependent protein kinase C-alpha. J Hepatol 2001;34:284-291.

45. Fava G, Alpini G, Rychlicki C, Saccomanno S, DeMorrow S, Trozzi L, Candelaresi C, et al. Leptin enhances cholangiocarcinoma cell growth. Cancer Res 2008;68:6752-6761.

46. Mancino A, Mancino MG, Glaser SS, Alpini G, Bolognese A, Izzo L, Francis H, et al. Estrogens stimulate the proliferation of human cholangiocarcinoma by inducing the expression and secretion of vascular endothelial growth factor. Dig Liver Dis 2009;41:156-163.

47. Reppert SM, Weaver DR. Coordination of circadian timing in mammals. Nature 2002;418:935-941.

48. Gooley JJ, Lu J, Chou TC, Scammell TE, Saper CB. Melanopsin in cells of origin of the retinohypothalamic tract. Nat Neurosci 2001;4:1165.

49. Ruby NF, Brennan TJ, Xie X, Cao V, Franken P, Heller HC, O'Hara BF. Role of melanopsin in circadian responses to light. Science 2002;298:2211-2213.

50. Liu C, Weaver DR, Strogatz SH, Reppert SM. Cellular construction of a circadian clock: period determination in the suprachiasmatic nuclei. Cell 1997;91:855-860.

51. Hansen J. Increased breast cancer risk among women who work predominantly at night. Epidemiology 2001;12:74-77.

52. Kubo T, Ozasa K, Mikami K, Wakai K, Fujino Y, Watanabe Y, Miki T, et al. Prospective cohort study of the risk of prostate cancer among rotating-shift workers: findings from the Japan collaborative cohort study. Am J Epidemiol 2006;164:549-555.

53. Schernhammer ES, Laden F, Speizer FE, Willett WC, Hunter DJ, Kawachi I, Fuchs CS, et al. Night-shift work and risk of colorectal cancer in the nurses' health study. J Natl Cancer Inst 2003;95:825-828.

54. Shearman LP, Sriram S, Weaver DR, Maywood ES, Chaves I, Zheng B, Kume K, et al. Interacting molecular loops in the mammalian circadian clock. Science 2000;288:1013-1019.

55. Savvidis C, Koutsilieris M. Circadian rhythm disruption in cancer biology. Mol Med 2012;18:1249-1260.

56. Bozek K, Relogio A, Kielbasa SM, Heine M, Dame C, Kramer A, Herzel H. Regulation of clock-controlled genes in mammals. PLoS One 2009;4:e4882.

57. Cheng HY, Papp JW, Varlamova O, Dziema H, Russell B, Curfman JP, Nakazawa T, et al. microRNA modulation of circadian-clock period and entrainment. Neuron 2007;54:813-829.

58. Kawamoto T, Noshiro M, Sato F, Maemura K, Takeda N, Nagai R, Iwata T, et al. A novel autofeedback loop of Dec1 transcription involved in circadian rhythm regulation. Biochem Biophys Res Commun 2004;313:117-124.

59. Kornmann B, Schaad O, Bujard H, Takahashi JS, Schibler U. System-driven and oscillator-dependent circadian transcription in mice with a conditionally active liver clock. PLoS Biol 2007;5:e34.

60. Ruiter M, La Fleur SE, van Heijningen C, van der Vliet J, Kalsbeek A, Buijs RM. The daily rhythm in plasma glucagon concentrations in the rat is

modulated by the biological clock and by feeding behavior. Diabetes 2003;52:1709-1715.

61. Ando H, Yanagihara H, Hayashi Y, Obi Y, Tsuruoka S, Takamura T, Kaneko S, et al. Rhythmic messenger ribonucleic acid expression of clock genes and adipocytokines in mouse visceral adipose tissue. Endocrinology 2005;146:5631-5636.

62. La Fleur SE, Kalsbeek A, Wortel J, Buijs RM. A suprachiasmatic nucleus generated rhythm in basal glucose concentrations. J Neuroendocrinol 1999;11:643-652.

63. Ahima RS, Prabakaran D, Flier JS. Postnatal leptin surge and regulation of circadian rhythm of leptin by feeding. Implications for energy homeostasis and neuroendocrine function. J Clin Invest 1998;101:1020-1027.

64. De Boer SF, Van der Gugten J. Daily variations in plasma noradrenaline, adrenaline and corticosterone concentrations in rats. Physiol Behav 1987;40:323-328.

65. Bodosi B, Gardi J, Hajdu I, Szentirmai E, Obal F, Jr., Krueger JM. Rhythms of ghrelin, leptin, and sleep in rats: effects of the normal diurnal cycle, restricted feeding, and sleep deprivation. Am J Physiol Regul Integr Comp Physiol 2004;287:R1071-1079.

66. Froy O. Metabolism and circadian rhythms--implications for obesity. Endocr Rev 2010;31:1-24.

67. Rudic RD, McNamara P, Curtis AM, Boston RC, Panda S, Hogenesch JB, Fitzgerald GA. BMAL1 and CLOCK, two essential components of the circadian clock, are involved in glucose homeostasis. PLoS Biol 2004;2:e377.

68. Yang S, Liu A, Weidenhammer A, Cooksey RC, McClain D, Kim MK, Aguilera G, et al. The role of mPer2 clock gene in glucocorticoid and feeding rhythms. Endocrinology 2009;150:2153-2160.

69. Stevens RG. Circadian disruption and breast cancer: from melatonin to clock genes. Epidemiology 2005;16:254-258.

70. Winter SL, Bosnoyan-Collins L, Pinnaduwage D, Andrulis IL. Expression of the circadian clock genes Per1 and Per2 in sporadic and familial breast tumors. Neoplasia 2007;9:797-800.

71. Kuo SJ, Chen ST, Yeh KT, Hou MF, Chang YS, Hsu NC, Chang JG. Disturbance of circadian gene expression in breast cancer. Virchows Arch 2009;454:467-474.

72. Cao Q, Gery S, Dashti A, Yin D, Zhou Y, Gu J, Koeffler HP. A role for the clock gene per1 in prostate cancer. Cancer Res 2009;69:7619-7625.

73. Filipski E, Subramanian P, Carriere J, Guettier C, Barbason H, Levi F. Circadian disruption accelerates liver carcinogenesis in mice. Mutat Res 2009;680:95-105.

74. Taniguchi H, Fernandez AF, Setien F, Ropero S, Ballestar E, Villanueva A, Yamamoto H, et al. Epigenetic inactivation of the circadian clock gene BMAL1 in hematologic malignancies. Cancer Res 2009;69:8447-8454.

75. Kettner NM, Katchy CA, Fu L. Circadian gene variants in cancer. Ann Med 2014;46:208-220.

76. Marcheva B, Ramsey KM, Buhr ED, Kobayashi Y, Su H, Ko CH, Ivanova G, et al. Disruption of the clock components CLOCK and BMAL1 leads to hypoinsulinaemia and diabetes. Nature 2010;466:627-631.

77. Geyfman M, Kumar V, Liu Q, Ruiz R, Gordon W, Espitia F, Cam E, et al. Brain and muscle Arnt-like protein-1 (BMAL1) controls circadian cell proliferation and susceptibility to UVB-induced DNA damage in the epidermis. Proc Natl Acad Sci U S A 2012;109:11758-11763.

78. Fu L, Kettner NM. The circadian clock in cancer development and therapy. Prog Mol Biol Transl Sci 2013;119:221-282.

79. Yang X, Wood PA, Ansell CM, Ohmori M, Oh EY, Xiong Y, Berger FG, et al. Beta-catenin induces beta-TrCP-mediated PER2 degradation altering circadian clock gene expression in intestinal mucosa of ApcMin/+ mice. J Biochem 2009;145:289-297.

80. Giacchetti S, Dugue PA, Innominato PF, Bjarnason GA, Focan C, Garufi C, Tumolo S, et al. Sex moderates circadian chemotherapy effects on survival of patients with metastatic colorectal cancer: a meta-analysis. Ann Oncol 2012;23:3110-3116.

81. Plikus MV, Vollmers C, de la Cruz D, Chaix A, Ramos R, Panda S, Chuong CM. Local circadian clock gates cell cycle progression of transient

amplifying cells during regenerative hair cycling. Proc Natl Acad Sci U S A 2013;110:E2106-2115.

82. Zhang Y, Chen X, Ren P, Su Z, Cao H, Zhou J, Zou X, et al. Synergistic effect of combination topotecan and chronomodulated radiation therapy on xenografted human nasopharyngeal carcinoma. Int J Radiat Oncol Biol Phys 2013;87:356-362.

83. Innominato PF, Roche VP, Palesh OG, Ulusakarya A, Spiegel D, Levi FA. The circadian timing system in clinical oncology. Ann Med 2014;46:191-207.

84. Lee RC, Feinbaum RL, Ambros V. The C. elegans heterochronic gene lin-4 encodes small RNAs with antisense complementarity to lin-14. Cell 1993;75:843-854.

85. Reinhart BJ, Slack FJ, Basson M, Pasquinelli AE, Bettinger JC, Rougvie AE, Horvitz HR, et al. The 21-nucleotide let-7 RNA regulates developmental timing in Caenorhabditis elegans. Nature 2000;403:901-906.

86. Di Leva G, Garofalo M, Croce CM. MicroRNAs in cancer. Annu Rev Pathol 2014;9:287-314.

87. Calin GA, Dumitru CD, Shimizu M, Bichi R, Zupo S, Noch E, Aldler H, et al. Frequent deletions and down-regulation of micro- RNA genes miR15 and miR16 at 13q14 in chronic lymphocytic leukemia. Proc Natl Acad Sci U S A 2002;99:15524-15529.

88. Meng F, Henson R, Wehbe-Janek H, Ghoshal K, Jacob ST, Patel T. MicroRNA-21 regulates expression of the PTEN tumor suppressor gene in human hepatocellular cancer. Gastroenterology 2007;133:647-658.

89. Trang P, Medina PP, Wiggins JF, Ruffino L, Kelnar K, Omotola M, Homer R, et al. Regression of murine lung tumors by the let-7 microRNA. Oncogene 2010;29:1580-1587.

90. Kota J, Chivukula RR, O'Donnell KA, Wentzel EA, Montgomery CL, Hwang HW, Chang TC, et al. Therapeutic microRNA delivery suppresses tumorigenesis in a murine liver cancer model. Cell 2009;137:1005-1017.

91. Macfarlane LA, Murphy PR. MicroRNA: Biogenesis, Function and Role in Cancer. Curr Genomics 2010;11:537-561.

92. Hossain A, Kuo MT, Saunders GF. Mir-17-5p regulates breast cancer cell proliferation by inhibiting translation of AIB1 mRNA. Mol Cell Biol 2006;26:8191-8201.

93. Calin GA, Croce CM. MicroRNA signatures in human cancers. Nat Rev Cancer 2006;6:857-866.

94. Gatfield D, Le Martelot G, Vejnar CE, Gerlach D, Schaad O, Fleury-Olela F, Ruskeepaa AL, et al. Integration of microRNA miR-122 in hepatic circadian gene expression. Genes Dev 2009;23:1313-1326.

95. Chen L, Tang Y, Wang J, Yan Z, Xu R. miR-421 induces cell proliferation and apoptosis resistance in human nasopharyngeal carcinoma via downregulation of FOXO4. Biochem Biophys Res Commun 2013;435:745-750.

96. Shen H, Zhu F, Liu J, Xu T, Pei D, Wang R, Qian Y, et al. Alteration in Mir-21/PTEN Expression Modulates Gefitinib Resistance in Non-Small Cell Lung Cancer. PLoS One 2014;9:e103305.

97. Slaby O, Svoboda M, Fabian P, Smerdova T, Knoflickova D, Bednarikova M, Nenutil R, et al. Altered expression of miR-21, miR-31, miR-143 and miR-145 is related to clinicopathologic features of colorectal cancer. Oncology 2007;72:397-402.

98. Wang N, Zhou Y, Zheng L, Li H. MiR-31 is an independent prognostic factor and functions as an oncomir in cervical cancer via targeting ARID1A. Gynecol Oncol 2014;134:129-137.

99. Zhang J, Han C, Wu T. MicroRNA-26a promotes cholangiocarcinoma growth by activating beta-catenin. Gastroenterology 2012;143:246-256 e248.

100. Haga H, Yan I, Takahashi K, Wood J, Patel T. Emerging insights into the role of microRNAs in the pathogenesis of cholangiocarcinoma. Gene Expr 2014;16:93-99.

101. He Q, Cai L, Shuai L, Li D, Wang C, Liu Y, Li X, et al. Ars2 is overexpressed in human cholangiocarcinomas and its depletion increases PTEN and PDCD4 by decreasing microRNA-21. Mol Carcinog 2013;52:286-296.

102. Du Y, Xu Y, Ding L, Yao H, Yu H, Zhou T, Si J. Down-regulation of miR-141 in gastric cancer and its involvement in cell growth. J Gastroenterol 2009;44:556-561.

103. Nakada C, Matsuura K, Tsukamoto Y, Tanigawa M, Yoshimoto T, Narimatsu T, Nguyen LT, et al. Genome-wide microRNA expression profiling in renal cell carcinoma: significant down-regulation of miR-141 and miR-200c. J Pathol 2008;216:418-427.

104. Banaudha K, Kaliszewski M, Korolnek T, Florea L, Yeung ML, Jeang KT, Kumar A. MicroRNA silencing of tumor suppressor DLC-1 promotes efficient hepatitis C virus replication in primary human hepatocytes. Hepatology 2011;53:53-61.

105. Zhao X, Yang L, Hu J, Ruan J. miR-138 might reverse multidrug resistance of leukemia cells. Leuk Res 2010;34:1078-1082.

106. Liu X, Lv XB, Wang XP, Sang Y, Xu S, Hu K, Wu M, et al. MiR-138 suppressed nasopharyngeal carcinoma growth and tumorigenesis by targeting the CCND1 oncogene. Cell Cycle 2012;11:2495-2506.

107. Wang W, Zhao LJ, Tan YX, Ren H, Qi ZT. MiR-138 induces cell cycle arrest by targeting cyclin D3 in hepatocellular carcinoma. Carcinogenesis 2012;33:1113-1120.

108. Zhao Y, Jia HL, Zhou HJ, Dong QZ, Fu LY, Yan ZW, Sun J, et al. [Identification of metastasis-related microRNAs of hepatocellular carcinoma in hepatocellular carcinoma cell lines by quantitative real time PCR]. Zhonghua Gan Zang Bing Za Zhi 2009;17:526-530.

109. Li R, Qian N, Tao K, You N, Wang X, Dou K. MicroRNAs involved in neoplastic transformation of liver cancer stem cells. J Exp Clin Cancer Res 2010;29:169.

110. Huang J, Wang Y, Guo Y, Sun S. Down-regulated microRNA-152 induces aberrant DNA methylation in hepatitis B virus-related hepatocellular carcinoma by targeting DNA methyltransferase 1. Hepatology 2010;52:60-70.

111. Chen L, Yan HX, Yang W, Hu L, Yu LX, Liu Q, Li L, et al. The role of microRNA expression pattern in human intrahepatic cholangiocarcinoma. J Hepatol 2009;50:358-369.

112. Braconi C, Huang N, Patel T. MicroRNA-dependent regulation of DNA methyltransferase-1 and tumor suppressor gene expression by interleukin-6 in human malignant cholangiocytes. Hepatology 2010;51:881-890.

113. Knuth A, Gabbert H, Dippold W, Klein O, Sachsse W, Bitter-Suermann D, Prellwitz W, et al. Biliary adenocarcinoma. Characterisation of three new human tumor cell lines. J Hepatol 1985;1:579-596.

114. Kusaka Y, Muraoka A, Tokiwa T, Sato J. Establishment and characterization of a human cholangiocellular carcinoma cell line. Hum Cell 1988;1:92-94.

115. Saijyo S, Kudo T, Suzuki M, Katayose Y, Shinoda M, Muto T, Fukuhara K, et al. Establishment of a new extrahepatic bile duct carcinoma cell line, TFK-1. Tohoku J Exp Med 1995;177:61-71.

116. Shimizu Y, Demetris AJ, Gollin SM, Storto PD, Bedford HM, Altarac S, Iwatsuki S, et al. Two new human cholangiocarcinoma cell lines and their cytogenetics and responses to growth factors, hormones, cytokines or immunologic effector cells. Int J Cancer 1992;52:252-260.

117. Miyagiwa M, Ichida T, Tokiwa T, Sato J, Sasaki H. A new human cholangiocellular carcinoma cell line (HuCC-T1) producing carbohydrate antigen 19/9 in serum-free medium. *In Vitro* Cell Dev Biol 1989;25:503-510.

118. Storto PD, Saidman SL, Demetris AJ, Letessier E, Whiteside TL, Gollin SM. Chromosomal breakpoints in cholangiocarcinoma cell lines. Genes Chromosomes Cancer 1990;2:300-310.

119. Grubman SA, Perrone RD, Lee DW, Murray SL, Rogers LC, Wolkoff LI, Mulberg AE, et al. Regulation of intracellular pH by immortalized human intrahepatic biliary epithelial cell lines. Am J Physiol Gastrointest Liver Physiol 1994;266:G1060-1070.

120. DeMorrow S, Glaser S, Francis H, Venter J, Vaculin B, Vaculin S, Alpini G. Opposing actions of endocannabinoids on cholangiocarcinoma growth: recruitment of Fas and Fas ligand to lipid rafts. J Biol Chem 2007;282:13098-13113.

121. Balsalobre A, Damiola F, Schibler U. A serum shock induces circadian gene expression in mammalian tissue culture cells. Cell 1998;93:929-937.

122. Han Y, Demorrow S, Invernizzi P, Jing Q, Glaser S, Renzi A, Meng F, et al. Melatonin exerts by an autocrine loop antiproliferative effects in

cholangiocarcinoma: its synthesis is reduced favoring cholangiocarcinoma growth. Am J Physiol Gastrointest Liver Physiol 2011;301:G623-633.

123. Vermes I, Haanen C, Steffens-Nakken H, Reutelingsperger C. A novel assay for apoptosis. Flow cytometric detection of phosphatidylserine expression on early apoptotic cells using fluorescein labelled Annexin V. J Immunol Methods 1995;184:39-51.

124. Yan D, Dong Xda E, Chen X, Wang L, Lu C, Wang J, Qu J, et al. MicroRNA-1/206 targets c-Met and inhibits rhabdomyosarcoma development. J Biol Chem 2009;284:29596-29604.

125. Maragkakis M, Alexiou P, Papadopoulos GL, Reczko M, Dalamagas T, Giannopoulos G, Goumas G, et al. Accurate microRNA target prediction correlates with protein repression levels. BMC Bioinformatics 2009;10:295.

126. Enright AJ, John B, Gaul U, Tuschl T, Sander C, Marks DS. MicroRNA targets in Drosophila. Genome Biol 2003;5:R1.

127. Rehmsmeier M, Steffen P, Hochsmann M, Giegerich R. Fast and effective prediction of microRNA/target duplexes. RNA 2004;10:1507-1517.

128. Tivnan A, Tracey L, Buckley PG, Alcock LC, Davidoff AM, Stallings RL. MicroRNA-34a is a potent tumor suppressor molecule in vivo in neuroblastoma. BMC Cancer 2011;11:33.

129. Guessous F, Zhang Y, Kofman A, Catania A, Li Y, Schiff D, Purow B, et al. microRNA-34a is tumor suppressive in brain tumors and glioma stem cells. Cell Cycle 2010;9:1031-1036.

130. Welch C, Chen Y, Stallings RL. MicroRNA-34a functions as a potential tumor suppressor by inducing apoptosis in neuroblastoma cells. Oncogene 2007;26:5017-5022.

131. Li N, Fu H, Tie Y, Hu Z, Kong W, Wu Y, Zheng X. miR-34a inhibits migration and invasion by down-regulation of c-Met expression in human hepatocellular carcinoma cells. Cancer Lett 2009;275:44-53.

132. Gery S, Komatsu N, Baldjyan L, Yu A, Koo D, Koeffler HP. The circadian gene per1 plays an important role in cell growth and DNA damage control in human cancer cells. Mol Cell 2006;22:375-382.

133. Kiem HP, Nourse J, Saltman DL, Blume KG, Cleary ML. Concurrent activation of c-myc and inactivation of bcl-2 by chromosomal translocation in a lymphoblastic lymphoma cell line. Oncogene 1990;5:1815-1819.

134. Buzzelli G, Dattolo P, Pinzani M, Brocchi A, Romano S, Gentilini P. Circulating growth hormone and insulin-like growth factor-I in nonalcoholic liver cirrhosis with or without superimposed hepatocarcinoma: evidence of an altered circadian rhythm. Am J Gastroenterol 1993;88:1744-1748.

135. Keith LG, Oleszczuk JJ, Laguens M. Circadian rhythm chaos: a new breast cancer marker. Int J Fertil Womens Med 2001;46:238-247.

136. Kloog I, Haim A, Stevens RG, Portnov BA. Global co-distribution of light at night (LAN) and cancers of prostate, colon, and lung in men. Chronobiol Int 2009;26:108-125.

137. Panzer A. Melatonin in osteosarcoma: an effective drug? Med Hypotheses 1997;48:523-525.

138. Reed VA. Shift work, light at night, and the risk of breast cancer. AAOHN J 2011;59:37-45; quiz 46.

139. Rich T, Innominato PF, Boerner J, Mormont MC, Iacobelli S, Baron B, Jasmin C, et al. Elevated serum cytokines correlated with altered behavior, serum cortisol rhythm, and dampened 24-hour rest-activity patterns in patients with metastatic colorectal cancer. Clin Cancer Res 2005;11:1757-1764.

140. Viswanathan AN, Hankinson SE, Schernhammer ES. Night shift work and the risk of endometrial cancer. Cancer Res 2007;67:10618-10622.

141. Kalsbeek A, la Fleur S, Fliers E. Circadian control of glucose metabolism. Mol Metab 2014;3:372-383.

142. Turek FW, Joshu C, Kohsaka A, Lin E, Ivanova G, McDearmon E, Laposky A, et al. Obesity and metabolic syndrome in circadian Clock mutant mice. Science 2005;308:1043-1045.

143. Kudo T, Kawashima M, Tamagawa T, Shibata S. Clock mutation facilitates accumulation of cholesterol in the liver of mice fed a cholesterol and/or cholic acid diet. Am J Physiol Endocrinol Metab 2008;294:E120-130.

144. Shimba S, Ogawa T, Hitosugi S, Ichihashi Y, Nakadaira Y, Kobayashi M, Tezuka M, et al. Deficient of a clock gene, brain and muscle Arnt-like protein-1 (BMAL1), induces dyslipidemia and ectopic fat formation. PLoS One 2011;6:e25231.

145. Mostafaie N, Kallay E, Sauerzapf E, Bonner E, Kriwanek S, Cross HS, Huber KR, et al. Correlated downregulation of estrogen receptor beta and the circadian clock gene Per1 in human colorectal cancer. Mol Carcinog 2009;48:642-647.

146. Yeh KT, Yang MY, Liu TC, Chen JC, Chan WL, Lin SF, Chang JG. Abnormal expression of period 1 (PER1) in endometrial carcinoma. J Pathol 2005;206:111-120.

147. Gery S, Komatsu N, Kawamata N, Miller CW, Desmond J, Virk RK, Marchevsky A, et al. Epigenetic silencing of the candidate tumor suppressor gene Per1 in non-small cell lung cancer. Clin Cancer Res 2007;13:1399-1404.

148. Chen ST, Choo KB, Hou MF, Yeh KT, Kuo SJ, Chang JG. Deregulated expression of the PER1, PER2 and PER3 genes in breast cancers. Carcinogenesis 2005;26:1241-1246.

149. Sato F, Nagata C, Liu Y, Suzuki T, Kondo J, Morohashi S, Imaizumi T, et al. PERIOD1 is an anti-apoptotic factor in human pancreatic and hepatic cancer cells. J Biochem 2009;146:833-838.

150. Takahashi JS, Hong HK, Ko CH, McDearmon EL. The genetics of mammalian circadian order and disorder: implications for physiology and disease. Nat Rev Genet 2008;9:764-775.

151. Storch KF, Lipan O, Leykin I, Viswanathan N, Davis FC, Wong WH, Weitz CJ. Extensive and divergent circadian gene expression in liver and heart. Nature 2002;417:78-83.

152. Liu K, Wang R. MicroRNA-mediated regulation in the mammalian circadian rhythm. J Theor Biol 2012;304:103-110.

153. Mormont MC, Levi F. Circadian-system alterations during cancer processes: a review. Int J Cancer 1997;70:241-247.

154. Han Y, Onori P, Meng F, DeMorrow S, Venter J, Francis H, Franchitto A, et al. Prolonged exposure of cholestatic rats to complete dark inhibits biliary hyperplasia and liver fibrosis. Am J Physiol Gastrointest Liver Physiol 2014.